

# Hybrid Full-/Half-Duplex System Analysis in Heterogeneous Wireless Networks

Jemin Lee, *Member, IEEE* and Tony Q. S. Quek, *Senior Member, IEEE*

**Abstract**—Full-duplex (FD) radio has been introduced for bidirectional communications on the same temporal and spectral resources so as to maximize spectral efficiency. In this paper, motivated by the recent advances in FD radios, we provide a foundation for hybrid-duplex heterogeneous networks (HDHNs), composed of multi-tier networks with a mixture of access points (APs), operating either in bidirectional FD mode or downlink half-duplex (HD) mode. Specifically, we characterize the network interference from FD-mode cells, and derive the HDHN throughput by accounting for AP spatial density, self-interference cancellation (IC) capability, and transmission power of APs and users. By quantifying the HDHN throughput, we present the effect of network parameters and the self-IC capability on the HDHN throughput, and show the superiority of FD mode for larger AP densities (i.e., larger network interference and shorter communication distance) or higher self-IC capability. Furthermore, our results show operating all APs in FD or HD achieves higher throughput compared to the mixture of two mode APs in each tier network, and introducing hybrid-duplex for different tier networks improves the heterogenous network throughput.

**Index Terms**—Heterogeneous networks, full-duplex, half-duplex, self-interference, network interference, stochastic geometry

## I. INTRODUCTION

Conventional communication systems operate in half-duplex (HD) such as time-division or frequency-division approaches, which require different orthogonal resources in either temporal or spectral domain for bidirectional communications. As a way of enhancing the spectral efficiency of communication systems, full-duplex (FD) has been introduced to perform bidirectional communications on the same temporal and spectral resources. Thus, FD radios can potentially be employed in heterogeneous networks for increased link capacity, more flexibility in spectrum usage, and improved communication security [1].

Different FD systems have been studied considering the asynchronous transmission and reception [2], the one-way relay transmission [3]–[5], the two-way relay transmission [3], [6], the imperfect channel estimation and limited dynamic range in a multiple-input multiple-output (MIMO) system [7],

and relays with different self-interference cancellation (IC) capabilities in multi-hop transmission [8]. The achievable rates of HD and FD in MIMO systems have been compared in [9], and the degree-of-freedom of the system with a FD base stations (BSs) with HD users has been analyzed by considering the intra-cell inter-node interference [10]. The FD radios has also been used in jamming techniques for communication secrecy [11] and bidirectional broadcast communications by implementing rapid on-off-division duplex [12]. The hybrid of FD- and HD-relaying schemes have also been presented, which allows a relay to opportunistically switch between two modes based on instantaneous [13]–[15] or statistical channel state information (CSI) [15].

The key challenging in implementing a FD radio is the presence of self-interference, received at a node from its own transmission while transmitting and receiving at the same time. Self-IC techniques for FD systems with multiple antennas have been proposed by exploiting the following domains: 1) propagation-domain schemes including antenna separation [16], [17] and directional transmit/receive antennas (e.g., beamforming-based techniques) [18]–[20]; 2) analog circuit-domain including channel-unaware schemes [16], [21] and channel-aware schemes [16], [22]–[24]; 3) digital circuit-domain [14], [15]; and 4) hybrid of analog and digital domains [25], [26]. The self-IC techniques are being researched actively as the current self-IC capability is still challengeable. Recently, the feasibility of single (shared)-array FD transceivers has also been presented in [24], [27], [28]. However, there is no work that considers the self-interference together with the network interference generated from randomly distributed FD-mode nodes for the performance evaluation of FD systems. If more nodes operate in FD, the number of communicating nodes in the network increases, but network interference also increases, which can degrade the communication reliability between nodes. The network interference from FD-mode nodes has been presented in [29], [30], but one tier network was considered with the perfect self-IC assumption.<sup>1</sup>

The performance of heterogeneous networks has been studied [31]–[44] by taking into account the spatial node distribution using the Poisson point process (PPP), which is widely used in wireless networks [45]–[51].<sup>2</sup> The heterogeneous

Manuscript received April 07, 2014; revised August 26, 2014 and November 5, 2014.

J. Lee and T. Q. S. Quek are with the Singapore University of Technology and Design, 8 Somapah Road, Singapore 487372 (e-mail: jmnlee@ieee.org, tonyquek@sutd.edu.sg). The material in this paper was presented, in part, at the Global Communications Conference, Austin, TX, Dec. 2014.

This research was supported, in part, by Temasek Research Fellowship, the SUTD-MIT International Design Centre under Grant IDSF1200106OH, and the A\*STAR SERC under Grant 1224104048.

<sup>1</sup>Furthermore, simpler network model was used in [29] by ignoring the intra-cell interference, which can be generated by users accessing the same resource in a cell, and the fixed link distance between a user and its communicating access point (AP) was used in [30].

<sup>2</sup>Recently, the PPP has also been used to evaluate some advanced techniques such as the coordinated multiple-point (CoMP) with BS-centric [52] and user-centric [53] clustering, and the self-powered transmitters using energy harvesting techniques [54].

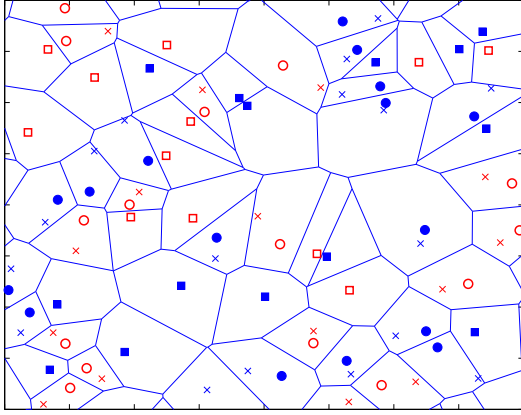


Fig. 1. An example of downlink two-tier HDHNs (squares, circles, crosses are HD-mode APs, FD-mode APs, and FD-mode users sharing the same channel in the first-tier network (empty red) and in the second-tier network (filled blue)).

network throughput has been presented by considering the  $K$ -tier spectrum sharing network in downlink [33] and in uplink [34], the BS loads of different tier networks [35], the interference cancellation capability [36], [37], the spectrum sharing methods [38], [39], and the trade-off between traffic offloading and energy consumption of small cells [40], [41]. To solve the load balancing problem in heterogeneous networks with HD systems, the concept of cell range expansion has also been considered to offload users to less loaded networks using a biased cell association rule [42], [43]. The design of duplex communication modes is also presented by considering the coordinated time-division duplexing (TDD) underlay structure in two-tier networks [55], and the hybrid division duplexing in the network composed of macro-cells in frequency-division duplexing (FDD) and cognitive femto-cells in TDD [44]. However, most of these works is based on HD and does not explore the effect of FD on network throughput, impeding the efficient duplex mode design for heterogeneous networks.

Motivated by the recent advances in FD radios, we propose the novel idea of hybrid-duplex cell networks for future heterogeneous cellular networks. We consider HDHNs, composed of multi-tier networks with a mixture of APs operating either in bidirectional FD mode or downlink HD mode. We develop a framework for HDHNs in the presence of self-interference and network interference. Specifically, after characterizing the network interference of HDHNs, we define a performance metric, namely the HDHN throughput, to measure the average data rate achieved by APs and users successfully communicating in this network. Based on this metric, we present the effect of network parameters such as the AP spatial density, the network interference, and the self-interference on the HDHN throughput. We then determine the portion of FD-mode APs that maximizes the HDHN throughput based on the system parameters including AP spatial density. Note that this is different from the opportunistic mode switching based on CSI in [13]–[15]. The main contributions of this paper can be summarized as follows:

TABLE I  
NOTATIONS USED THROUGHOUT THE PAPER.

Notation	Definition
$\Pi_{a,k}$	PPP for AP distribution of network $k$
$\Pi_{a,k}^m$	PPP for $m$ -mode AP distribution in network $k$
$\lambda_k$	Spatial density of APs of network $k$
$\lambda_k^m$	Spatial density of $m$ -mode APs in network $k$
$T_s$	Symbol time
$W$	Communication bandwidth
$H_{x,y}$	Fading level of the link between nodes at $\mathbf{x}$ and $\mathbf{y}$
$D_{x,y}$	Distance of the link between nodes at $\mathbf{x}$ and $\mathbf{y}$
$D_k^m$	Distance of the link between an user and its associated $m$ -mode AP in network $k$
$\alpha_k$	Pathloss exponent in network $k$
$\mathcal{W}_k$	Weighting factor of network $k$
$\mathcal{B}_{i,k}$	Ratio between association factors, $\mathcal{W}_i/\mathcal{W}_k$
$P_{a,k}$	Transmission power of a AP in network $k$
$P_{u,k}$	Transmission power of a user in network $k$
$P_r$	Transmission power at a receiving node
$I_k^m$	Interference from $m$ -mode APs in network $k$
$\gamma_k^m$	SIR at $m$ -mode node in network $k$
$\tau$	Target SIR
$C_k^m(P_r)$	Self-IC capability of $m$ -mode node in network $k$
$p_k^{\text{FD}}$	Portion of FD-mode APs in network $k$
$p_{S,k}^m$	Successful transmission probability of $m$ -mode node
$\mathcal{S}$	HDHN throughput [bits/sec/Hz/m <sup>2</sup> ]
$\mathcal{S}_k$	HDHN throughput of network $k$ [bits/sec/Hz/m <sup>2</sup> ]
$\mathcal{S}^c$	Cell throughput of HDHNs [bits/sec/Hz/cell]

- we characterize the network interference generating from distributed APs and users in FD-mode cells;
- we introduce and derive the HDHN throughput that accounts for self-interference, spatial AP densities, and transmission power of APs and users; and
- we quantify the HDHN throughput and present the optimal portion of FD-mode APs to maximize the HDHN throughput according to the self-IC capability and network parameters.

The remainder of this paper is organized as follows: Section II describes the HDHN model and provides the statistical characterization of interference from FD-mode cells. Section III analyzes the successful transmission probability of HDHNs, and introduces and analyzes the HDHN throughput. Section IV quantifies the effects of network parameters and self-interference capability on the HDHN throughput and determines the optimal portion of FD-mode APs in HDHNs. Finally, conclusions are given in Section V.

*Notation:* The notation used throughout the paper is reported in Table I.

## II. HYBRID-DUPLEX HETEROGENEOUS NETWORK MODEL

In this section, we describe the HDHN model and characterize the network interference of the HDHN.

### A. Network Model

We consider HDHNs composed of  $K$ -tier wireless networks. The  $k$ th-tier network consists of APs distributed in space according to a homogeneous PPP  $\Pi_{a,k}$  with spatial density  $\lambda_k$ . Each AP forms a cell and communicates to nodes in either downlink HD mode or bidirectional FD mode. The portion of FD-mode APs in the  $k$ th-tier network is  $p_k^{\text{FD}}$ , and the distributions of HD-mode and FD-mode APs also follow PPPs,  $\Pi_{a,k}^{\text{HD}}$  and  $\Pi_{a,k}^{\text{FD}}$ , with spatial densities  $\lambda_k^{\text{HD}} = \lambda_k(1 - p_k^{\text{FD}})$  and  $\lambda_k^{\text{FD}} = \lambda_k p_k^{\text{FD}}$ , respectively. All HD-mode cells are in downlink while all FD-mode cells have both uplink and downlink communications. In the HDHNs, users in FD-mode cells and all APs of the  $k$ th-tier network transmit with power  $P_{u,k}$  and  $P_{a,k}$ , respectively, and generally  $P_{a,k} \geq P_{u,k}$ . Each channel is used by one user in a cell to avoid intra-cell interference, and the whole spectrum is utilized in each cell.<sup>3</sup> An example of downlink HDHNs is presented in Fig. 1.

Users are scattered in HDHNs according to a homogeneous PPP  $\Pi_u$  with spatial density  $\mu$ , and a node located at  $\mathbf{x}_o$  connects to an AP in the  $k$ -tier networks based on the association rule, presented by [43]

$$k = \arg \max_{i \in \mathcal{K}} \left\{ \max_{\mathbf{X}_i \in \Pi_{a,i}} \mathcal{W}_i D_{\mathbf{X}_i, \mathbf{x}_o}^{-\alpha_i} \right\} \quad (1)$$

where  $\mathcal{K} = \{1, 2, \dots, K\}$  is the index set of  $K$  tier networks;  $\mathcal{W}_i$  is the weighting factor for the  $i$ th-tier network;  $D_{\mathbf{y}, \mathbf{x}}$  is the distance between nodes at  $\mathbf{y}$  and  $\mathbf{x}$ ; and  $\alpha_i > 2$  is the pathloss exponent in the  $i$ th-tier network. This association rule can be extended to special cases such as the rule that makes nodes associate to the nearest AP, i.e.,  $\mathcal{W}_i = 1$ , or to the AP providing the maximum average received power, i.e.,  $\mathcal{W}_i = P_{a,i} \mathcal{U}_i$  where  $\mathcal{U}_i$  is the association bias of the  $i$ th-tier network. Let us denote  $D_i^m$  as the distance to the  $m$ -mode AP with the maximum  $\mathcal{W}_i D_{\mathbf{X}_i, \mathbf{x}_o}^{-\alpha_i}$  for all  $\mathbf{X}_i \in \Pi_{a,i}^m$ . Using the association rule and  $D_i^m$ , the probability that a user is associated to an  $m$ -mode AP in the  $k$ th-tier network is given by

$$\begin{aligned} p_{A,k}^m &= \mathbb{P} \left\{ \bigcup_{i \in \mathcal{K}, m_o \in \{\text{FD}, \text{HD}\}} \mathcal{W}_k (D_k^m)^{-\alpha_k} > \mathcal{W}_i (D_i^{m_o})^{-\alpha_i} \right\} \\ &\stackrel{(a)}{=} 2\pi \lambda_k^m \int_0^\infty x \exp \left\{ -\pi \sum_{i \in \mathcal{K}, m_o \in \{\text{FD}, \text{HD}\}} \lambda_i^{m_o} \mathcal{B}_{ik}^{2/\alpha_i} x^{2\alpha_k/\alpha_i} \right\} dx \\ &= 2\pi \lambda_k^m \int_0^\infty x \exp \left\{ -\pi \sum_{i \in \mathcal{K}} \lambda_i \mathcal{B}_{ik}^{2/\alpha_i} x^{2\alpha_k/\alpha_i} \right\} dx \quad (2) \end{aligned}$$

where (a) is from Lemma 4 in [43], and  $\mathcal{B}_{ik} = \mathcal{W}_i/\mathcal{W}_k$  is the ratio between the association factor. Using (2), for a node associated to  $m$ -mode AP in the  $k$ th-tier network, the

probability distribution function (PDF) of the link distance to the associated AP,  $D_k^m$ , is given by [43]

$$\begin{aligned} f_{D_k^m}(x) &= \frac{2\pi \lambda_k^m x}{p_{A,k}^m} \exp \left\{ -\pi \sum_{i \in \mathcal{K}} \lambda_i \mathcal{B}_{ik}^{2/\alpha_i} x^{2\alpha_k/\alpha_i} \right\} \\ &= \frac{x \exp \left\{ -\pi \sum_{i \in \mathcal{K}} \lambda_i \mathcal{B}_{ik}^{2/\alpha_i} x^{2\alpha_k/\alpha_i} \right\}}{\int_0^\infty y \exp \left\{ -\pi \sum_{i \in \mathcal{K}} \lambda_i \mathcal{B}_{ik}^{2/\alpha_i} y^{2\alpha_k/\alpha_i} \right\} dy}. \quad (3) \end{aligned}$$

Note that  $D_k^m$  depends not on the spatial density  $\lambda_k^m$ , but on the sum of scaled spatial densities, i.e.,  $\sum_{i \in \mathcal{K}} \lambda_i (\mathcal{W}_i/\mathcal{W}_k)^{2/\alpha_i} x^{2\alpha_k/\alpha_i}$ .

All users and APs have a single antenna, and they are transmitting and receiving at the same time in FD mode [27], [28]. A node in FD mode receives self-interference from its transmitted signal, and performs IC for the self-interference. Since the amount of self-interference depends on the transmission power at the receiver  $P_r$  [27], we define the residual self-interference power after performing cancellation as [14], [15], [19]

$$C_k^m(P_r) = P_r H_{R,k} \quad (4)$$

for  $\forall k \in \mathcal{K}$  and  $\forall m \in \{\text{FD}, \text{HD}\}$ . Here,  $H_{R,k} = |h_{R,k}|^2$  shows the *self-IC capability* of nodes where  $h_{R,k}$  is the residual self-interfering channel of a node in the  $k$ th-tier network. In (4),  $C_k^{\text{FD}}(P_r) = 0$  denotes perfect self-IC, and  $C_k^{\text{HD}}(P_r) = 0$  since HD-mode nodes are not transmitting while receiving data.

The residual self-interfering channel gain  $H_{R,k}$  in (4) needs to be characterized according to cancellation algorithms. For instance, after a digital-domain cancellation,  $h_{R,k}$  can be presented as  $h_{R,k} = h_{S,k} - \hat{h}_{S,k}$  where  $h_{S,k}$  and  $\hat{h}_{S,k}$  are the self-interfering channel and its estimate as the self-interference is subtracted using its estimate [14], [19], [56], [57]. Then,  $H_{R,k}$  can be modeled as a constant value such as  $H_{R,k} = \sigma_c^2$  for the estimation error variance  $\sigma_c^2$  [14], [56], [57]. However, for other cancellation techniques such as analog-domain schemes [16], [21]–[24], propagation-domain schemes [17]–[20], and combined schemes of different domains [25], [26], the modeling of  $H_{R,k}$  is a still challenging problem. Hence, the parameterization of the self-IC capability in (4) can make the analysis more generic. We consider  $H_{R,k}$  as a constant value in this paper, but note that the analysis can be easily extended for the case of random  $H_{R,k}$  within our framework.<sup>4</sup>

### B. Network Interference Characterization

In the  $k$ th-tier HDHN, the signal-to-interference ratio (SIR) received by a node at  $\mathbf{x}_o$  from a transmitter at  $\mathbf{y}_o$  for a propagation channel model with pathloss and Rayleigh fading is defined as

$$\gamma_k^m = \frac{P_t H_{\mathbf{x}_o, \mathbf{y}_o} D_{\mathbf{x}_o, \mathbf{y}_o}^{-\alpha_k}}{C_k^m(P_r) + \sum_{i \in \mathcal{K}} (I_i^{\text{HD}} + I_{o,i}^{\text{FD}})} \quad (5)$$

where  $P_t$  is the transmission power at the transmitter,  $P_r$  is the transmission power at the receiver, and  $H_{\mathbf{x}_o, \mathbf{y}_o}$  is the i.i.d.

<sup>3</sup>Note that if channels are not always used in every cells, it only affects the spatial density of interfering nodes in the same framework of this paper.

<sup>4</sup>For instance, once the PDF of  $H_{R,k}$  is available for a certain self-IC algorithm, by averaging analytic results of the paper over the distribution of  $H_{R,k}$ , the results for the random  $H_{R,k}$  can be obtained.

$$\mathcal{L}_{I_i^{\text{FD}}}(s) = \begin{cases} \exp \left\{ -\pi \lambda_i^{\text{FD}} \left[ -\hat{D}^2 + s^{2/\alpha_i} \frac{2}{\alpha_i} \frac{1}{P_{u,i} - P_{a,i}} \left\{ \pi \csc \left( \frac{2\pi}{\alpha_i} \right) \left( P_{u,i}^{\frac{2}{\alpha_i}+1} - P_{a,i}^{\frac{2}{\alpha_i}+1} \right) \right. \right. \right. \\ \left. \left. \left. + \mathcal{I}_1 \left( \frac{2}{\alpha_i} + 1, \frac{1}{P_{u,i}}, \frac{-2}{\alpha_i}, \frac{s}{\hat{D}^{\alpha_i}} \right) - \mathcal{I}_1 \left( \frac{2}{\alpha_i} + 1, \frac{1}{P_{a,i}}, \frac{-2}{\alpha_i}, \frac{s}{\hat{D}^{\alpha_i}} \right) \right\} \right] \right\}, \text{ if } P_{a,i} \neq P_{u,i}, \\ \exp \left\{ -\pi \lambda_i^{\text{FD}} \left[ -\hat{D}^2 + \frac{2s^{2/\alpha_i}}{\alpha_i P_{a,i}^2} \left\{ P_{a,i}^{\frac{2}{\alpha_i}+2} \left( 1 + \frac{2}{\alpha_i} \right) \pi \csc \left( \frac{2\pi}{\alpha_i} \right) + \mathcal{I}_1 \left( \frac{2}{\alpha_i} + 2, \frac{1}{P_{a,i}}, \frac{-2}{\alpha_i}, \frac{s}{\hat{D}^{\alpha_i}} \right) \right\} \right] \right\}, \text{ otherwise.} \end{cases} \quad (13)$$

fading channel gain of the link, i.e.,  $H_{\mathbf{x}_o, \mathbf{y}_o} \sim \exp(1)$ . In (5), when a user at  $\mathbf{x}$  associates to an AP at  $\mathbf{y}$ ,  $I_i^{\text{HD}}$  and  $I_{o,i}^{\text{FD}}$  are the aggregate interference received from HD-mode cells and FD-mode cells in the  $i$ th-tier network, given by

$$I_i^{\text{HD}} = \sum_{\mathbf{z} \in \Pi_{a,i}^{\text{HD}}/\{\mathbf{y}\}} P_{a,i} H_{\mathbf{x}, \mathbf{z}} D_{\mathbf{x}, \mathbf{z}}^{-\alpha_i} \quad (6)$$

$$I_{o,i}^{\text{FD}} = \sum_{\mathbf{z} \in \Pi_{a,i}^{\text{FD}}/\{\mathbf{y}\}} P_{a,i} H_{\mathbf{x}, \mathbf{z}} D_{\mathbf{x}, \mathbf{z}}^{-\alpha_i} + P_{u,i} H_{\mathbf{x}, \mathbf{z} + N(\mathbf{z})} D_{\mathbf{x}, \mathbf{z} + N(\mathbf{z})}^{-\alpha_i} \quad (7)$$

where  $N(\mathbf{z})$  is the relative location of a user to its associated AP at  $\mathbf{z}$ . Note that in (7), interference from a FD-mode cell consists of the interference from an AP and a user.

Let us consider a user at  $\mathbf{x}$ , its associating AP at  $\mathbf{y}$ , the other APs at  $\mathbf{z} \in \Pi_{a,i}^{\text{FD}}/\{\mathbf{y}\}$ , and their associated users at  $\mathbf{z} + N(\mathbf{z})$ . Generally, the distance between  $\mathbf{x}$  and  $\mathbf{z}$  is greater than the distance between  $\mathbf{z}$  and  $\mathbf{z} + N(\mathbf{z})$ , i.e.,  $\|\mathbf{x} - \mathbf{z}\| \gg \|N(\mathbf{z})\|$ . Hence, due to the difficulty in obtaining the exact characteristics of  $I_i^{\text{FD}}$ , we assume that the distance between a user at  $\mathbf{x}$  and a user at  $\mathbf{z} + N(\mathbf{z})$  can be approximated to the distance between a user at  $\mathbf{x}$  and the unassociated AP at  $\mathbf{z}$  as<sup>5</sup>

$$D_{\mathbf{x}, \mathbf{z} + N(\mathbf{z})} \approx D_{\mathbf{x}, \mathbf{z}}. \quad (8)$$

Using the approximation in (8), the interference received from FD-mode cells can be presented as

$$I_i^{\text{FD}} = \sum_{\mathbf{z} \in \Pi_{a,i}^{\text{FD}}/\{\mathbf{y}\}} G_i D_{\mathbf{x}, \mathbf{z}}^{-\alpha_i} \quad (9)$$

where  $G_i$  is given by

$$G_i = P_{a,i} H_{\mathbf{x}, \mathbf{z}} + P_{u,i} H_{\mathbf{x}, \mathbf{z} + N(\mathbf{z})}. \quad (10)$$

In (10), if  $P_{a,i} = P_{u,i}$ ,  $G_i$  is the sum of two exponential random variables all with same rate  $P_{a,i}^{-1}$  and it follows the Erlang distribution [58]. On the other hand, if  $P_{a,i} \neq P_{u,i}$ ,  $G_i$  is the sum of two exponential random variables with different rates  $P_{a,i}^{-1}$  and  $P_{u,i}^{-1}$  and it follows the hypo-exponential distribution [58]. Hence, the PDF of  $G_i$  is given by [58]

$$p_{G_i}(x) = \begin{cases} \frac{1}{P_{a,i}^2} x e^{-x/P_{a,i}}, & \text{if } P_{a,i} = P_{u,i}, \\ \frac{e^{-x/P_{u,i}} - e^{-x/P_{a,i}}}{P_{u,i} - P_{a,i}}, & \text{otherwise} \end{cases} \quad (11)$$

<sup>5</sup>From the law of cosines, we have  $\|\mathbf{x} - (\mathbf{z} + N(\mathbf{z}))\|^2 \approx \|\mathbf{x} - \mathbf{z}\|^2$  for  $\|\mathbf{x} - \mathbf{z}\| \gg \|N(\mathbf{z})\|$ .

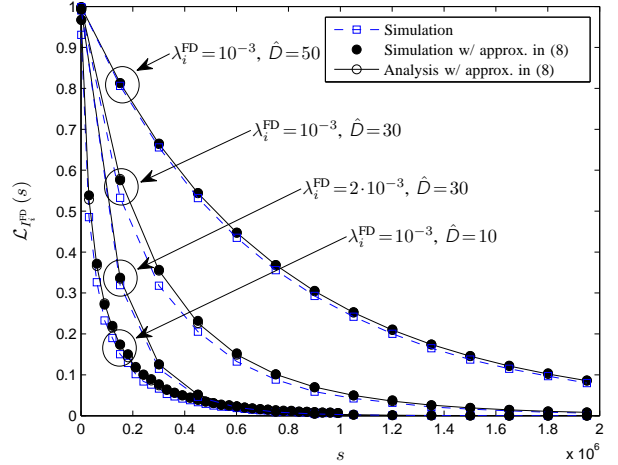


Fig. 2. An example of Laplace transform of network interference from FD-mode cells in the  $i$ th-tier network.

and we have<sup>6</sup>

$$\mathbb{E}_{G_i}\{G_i^\delta\} = \begin{cases} P_{a,i}^\delta \Gamma(2 + \delta), & \text{if } P_{a,i} = P_{u,i}, \\ \frac{\Gamma(1 + \delta) (P_{u,i}^{\delta+1} - P_{a,i}^{\delta+1})}{P_{u,i} - P_{a,i}}, & \text{otherwise} \end{cases} \quad (12)$$

for  $\delta > -1$  and the gamma function  $\Gamma(\cdot)$ . With the approximation in (8), we now obtain the Laplace transform of  $I_i^{\text{FD}}$  as follows.

*Lemma 1:* The Laplace transform of the approximated interference received from FD-mode cells in the  $i$ th-tier network,  $I_i^{\text{FD}}$  in (9), is given by (13) (on top of the page) where  $\hat{D}$  is the minimum distance to an interfering node and  $\mathcal{I}_1(x, y, z, \nu)$  is defined by

$$\begin{aligned} \mathcal{I}_1(x, y, z, \nu) &= \int_0^\infty t^{x-1} e^{-yt} \Gamma(z, \nu t) dt \\ &= \frac{\nu^z \Gamma(x+z)}{x(y+\nu)^{x+z}} {}_2F_1\left(1, x+z; x+1; \frac{y}{y+\nu}\right) \end{aligned} \quad (14)$$

for all constants  $\nu + y > 0$ ,  $y > 0$ , and  $x + z > 0$ ,  $\Gamma(\cdot, \cdot)$  is the upper incomplete function, and  ${}_2F_1(\cdot, \cdot; \cdot; \cdot)$  is the hypergeometric function.

*Proof:* See Appendix A. ■

<sup>6</sup>From (11),  $\mathbb{E}_{G_i}\{G_i^\delta\} = \int_0^\infty x^\delta p_{G_i}(x) dx$  can be obtained by substituting  $x/P_{a,i}$  (or  $x/P_{u,i}$ ) to  $y$  and using the Gamma function  $\Gamma(t) = \int_0^\infty y^{t-1} e^{-y} dy$ .

$$\tilde{\sigma}_{ik}(\alpha, P_t) = \begin{cases} \frac{-\mathcal{B}_{ik}^{2/\alpha}}{2} + \frac{P_t^{-2/\alpha} \tau^{2/\alpha}}{\alpha (P_{u,i} - P_{a,i})} \left[ \pi \csc\left(\frac{2\pi}{\alpha}\right) (P_{u,i}^{2/\alpha+1} - P_{a,i}^{2/\alpha+1}) \right. \\ \left. + \mathcal{I}_1\left(\frac{2}{\alpha} + 1, \frac{1}{P_{u,i}}, \frac{-2}{\alpha}, \frac{\tau}{P_t \mathcal{B}_{ik}}\right) - \mathcal{I}_1\left(\frac{2}{\alpha} + 1, \frac{1}{P_{a,i}}, \frac{-2}{\alpha}, \frac{\tau}{P_t \mathcal{B}_{ik}}\right) \right], & \text{if } P_{u,i} \neq P_{a,i}, \\ \frac{-\mathcal{B}_{ik}^{2/\alpha}}{2} + \frac{P_t^{-2/\alpha} \tau^{2/\alpha}}{\alpha P_{a,i}^2} \left[ P_{a,i}^{2/\alpha+2} \left(1 + \frac{2}{\alpha}\right) \pi \csc\left(\frac{2\pi}{\alpha}\right) + \mathcal{I}_1\left(\frac{2}{\alpha} + 2, \frac{1}{P_{a,i}}, \frac{-2}{\alpha}, \frac{\tau}{P_t \mathcal{B}_{ik}}\right) \right], & \text{otherwise.} \end{cases} \quad (17)$$

An example of the Laplace transform of  $I_i^{\text{FD}}$  is presented in Fig. 2 when the association policy in (1) is applied. For other parameters, the values presented in Table II are used. Fig. 2 shows a good match between the cases with and without the approximation in (8), especially for dense networks, i.e., large  $\lambda_i^{\text{FD}}$ .

Note that the Laplace transform of interference from FD-mode cells in Lemma 1 and the following analytical results related to FD mode can also be used when each FD-mode node has two antennas, one for transmitting and the other for receiving. In this case, the self-IC capability will be determined differently to the case of single antenna.

### III. HYBRID-DUPLEX HETEROGENEOUS NETWORK THROUGHPUT

In this section, we analyze the successful transmission probability of HDHNs, and define and derive the HDHN throughput as a new performance measurement for HDHNs.

#### A. Successful Transmission Probability

In this subsection, we analyze the successful transmission probability of HDHNs. We present the successful transmission probability of a  $m$ -mode node in the  $k$ th-tier network as  $p_{S,k}^m(\tau) = \mathbb{P}\{\gamma_k^m \geq \tau\}$ , where  $\tau$  is the target SIR value. Users and APs may have different target data rates such as  $R_u$  and  $R_a$ , respectively. In this case, the target SIRs of user and AP can be set to  $\tau_u = 2^{R_u/W} - 1$  and  $\tau_a = 2^{R_a/W} - 1$ , respectively, where  $W$  is a communication bandwidth. The  $p_{S,k}^m(\tau)$  is derived as follows.

*Theorem 1:* In HDHNs, the successful transmission probability of a  $m$ -mode node ( $m \in \{\text{HD}, \text{FD}\}$ ) in the  $k$ th-tier network is given by

$$p_{S,k}^m(P_t, P_r, \tau) = 2\pi \sum_{t \in \mathcal{K}} \lambda_t \mathcal{B}_{tk}^{2/\alpha_t} \times \int_0^\infty r \exp\left\{-\frac{r^{\alpha_k} \mathcal{C}_k^m(P_r) \tau}{P_t} - \sum_{i \in \mathcal{K}} r^{2\alpha_k/\alpha_i} 2\pi \lambda_i \zeta_{ik}(\alpha_i, P_t)\right\} dr \quad (15)$$

where  $P_t$  and  $P_r$  are the transmission power of the transmitter and the receiver, respectively. In (15),  $\zeta_{ik}(\alpha, P_t)$  is given by

$$\zeta_{ik}(\alpha, P_t) = \frac{\mathcal{B}_{ik}^{2/\alpha}}{2} + (1 - p_i^{\text{FD}}) \sigma_{ik}(\alpha, P_t) + p_i^{\text{FD}} \tilde{\sigma}_{ik}(\alpha, P_t) \quad (16)$$

<sup>7</sup>Note that  $\mathcal{L}_{I_i^{\text{FD}}}(s)$  can be extended to the case with transmission power control for  $P_{u,i}$  or  $P_{a,i}$  such as [34] by taking expectation to the exponential exponent in (36) according to the power distribution.

where  $\tilde{\sigma}_{ik}(\alpha, P_t)$  is given by (17) (on top of the page) and  $\sigma_{ik}(\alpha, P_t)$  is defined as

$$\sigma_{ik}(\alpha, P_t) = \mathcal{I}_0\left(1, \frac{P_t}{P_{a,i} \tau}, \mathcal{B}_{ik}, \alpha\right). \quad (18)$$

Here,  $\mathcal{I}_1(x, y, z, \nu)$  is defined in (14) and  $\mathcal{I}_0(x, y, z, \nu)$  is defined as

$$\begin{aligned} \mathcal{I}_0(x, y, z, \nu) &= \int_{(xz)^{1/\nu}}^\infty \frac{t}{x^{2/\nu}(1+y/xt^\nu)} dt \\ &= \frac{z^{2/\nu-1}}{(\nu-2)y} {}_2F_1\left(1, 1 - \frac{2}{\nu}; 2 - \frac{2}{\nu}; \frac{-1}{zy}\right) \end{aligned} \quad (19)$$

for all constants  $\nu > 2$  and  $x, y, z > 0$ .

*Proof:* See Appendix B. ■

The successful transmission probability  $p_{S,k}^m(P_t, P_r, \tau)$  in (15) also presents the portion of  $m$ -mode nodes or APs satisfying target data rate in the  $k$ th-tier network. The  $p_{S,k}^m(P_t, P_r, \tau)$  in (15) is difficult to be presented in a closed form, except for the cases of  $\alpha_i = 4, \forall i \in \mathcal{K}$  or  $\mathcal{C}_k^{\text{FD}}(P_r) = 0$ . The successful transmission probabilities are provided in closed forms for those special cases in the following corollaries.

*Corollary 1:* For  $\alpha_i = 4, \forall i \in \mathcal{K}$ , the successful transmission probability of a FD-mode node in the  $k$ th-tier network  $p_{S,k}^{\text{FD}}(P_t, P_r, \tau)$  is given by

$$\begin{aligned} p_{S,k}^{\text{FD}}(P_t, P_r, \tau) &= \frac{\pi^{3/2} \sqrt{P_t} \sum_{t \in \mathcal{K}} \lambda_t \mathcal{B}_{tk}^{1/2}}{2 \sqrt{\mathcal{C}_k^{\text{FD}}(P_r) \tau}} \\ &\times \exp\left\{\left(\frac{\pi \sqrt{P_t} \sum_{i \in \mathcal{K}} \lambda_i \zeta_{ik}(4, P_t)}{\sqrt{\mathcal{C}_k^{\text{FD}}(P_r) \tau}}\right)^2\right\} \\ &\times \text{Erfc}\left(\frac{\pi \sqrt{P_t} \sum_{i \in \mathcal{K}} \lambda_i \zeta_{ik}(4, P_t)}{\sqrt{\mathcal{C}_k^{\text{FD}}(P_r) \tau}}\right) \end{aligned} \quad (20)$$

where  $\zeta_{ik}(\alpha, P_t)$  is defined in (16) and  $\text{Erfc}(x) = \frac{2}{\sqrt{\pi}} \int_x^\infty e^{-t^2} dt$  is the complementary error function.

*Proof:* When  $\alpha_i = 4, \forall i \in \mathcal{K}$ , we can present  $p_{S,k}^m(P_t, P_r, \tau)$  in (15) as

$$\begin{aligned} p_{S,k}^m(P_t, P_r, \tau) &= 2\pi \sum_{t \in \mathcal{K}} \lambda_t \mathcal{B}_{tk}^{2/\alpha} \int_0^\infty r \exp\left\{-r^\alpha \frac{\mathcal{C}_k^m(P_r) \tau}{P_t} \right. \\ &\left. - r^2 \sum_{i \in \mathcal{K}} 2\pi \lambda_i \zeta_{ik}(\alpha, P_t)\right\} dr. \end{aligned} \quad (21)$$

For  $\alpha = 4$ , by substituting  $r^2$  with  $t$  in (21), we have

$$p_{S,k}^m(P_t, P_r, \tau) = \pi \sum_{t \in \mathcal{K}} \lambda_t \mathcal{B}_{tk}^{2/\alpha} \int_0^\infty \exp \left\{ -t^2 \frac{C_k^m(P_r) \tau}{P_t} - t \sum_{i \in \mathcal{K}} 2\pi \lambda_i \zeta_{ik}(\alpha, P_t) \right\} dt. \quad (22)$$

which results in (20) by [59, eq. (3.322)].  $\blacksquare$

*Corollary 2:* For  $\alpha_i = \alpha > 2$ ,  $\forall i \in \mathcal{K}$ , when the self-IC is perfect, i.e.,  $C_k^{\text{FD}}(P_r) = 0$ , the successful transmission probability of a FD-mode node in the  $k$ th-tier network  $p_{S,k}^{\text{FD}}(P_t, P_r, \tau)$  is given by

$$p_{S,k}^{\text{FD}}(P_t, P_r, \tau) = \frac{\sum_{i \in \mathcal{K}} \lambda_i \mathcal{B}_{ik}^{2/\alpha}}{2 \sum_{i \in \mathcal{K}} \lambda_i \zeta_{ik}(\alpha, P_t)} \quad (23)$$

where  $\zeta_{ik}(\alpha, P_t)$  is defined in (16).

*Proof:* When  $C_k^{\text{FD}}(P_r) = 0$  and  $\alpha_i = \alpha$ ,  $\forall i \in \mathcal{K}$ , from (21), we have

$$p_{S,k}^{\text{FD}}(P_t, P_r, \tau) = 2\pi \sum_{i \in \mathcal{K}} \lambda_i \mathcal{B}_{ik}^{2/\alpha} \times \int_0^\infty r \exp \left\{ -r^2 \sum_{i \in \mathcal{K}} 2\pi \lambda_i \zeta_{ik}(\alpha, P_t) \right\} dr \quad (24)$$

which results in (23).  $\blacksquare$

In HD mode, there is no self-interference (i.e.,  $C_k^{\text{HD}}(P_r) = 0$ ), so for  $\alpha_i = \alpha > 2$ ,  $\forall i \in \mathcal{K}$ , the successful transmission probability in  $k$ th-tier network can also be obtained from (24) as

$$p_{S,k}^{\text{HD}}(P_{a,k}, 0, \tau) = p_{S,k}^{\text{FD}}(P_{a,k}, 0, \tau) \quad (25)$$

where  $p_{S,k}^{\text{FD}}(P_t, P_r, \tau)$  is defined in (23).

## B. HDHN Throughput Analysis

In this subsection, we derive the HDHN throughput for various network settings. We first define the HDHN throughput as follows.

*Definition 1:* The HDHN throughput is defined by

$$\mathcal{S} = \frac{1}{W |\mathcal{A}|} \mathbb{E} \left\{ \sum_{k=1}^K \left[ \sum_{\mathbf{X} \in \Pi_{a,k}^{\text{HD}} \cap \mathcal{A}} R_a \mathbb{1}_{\mathcal{T}_k^{\text{HD}}(\mathbf{X}, \mathcal{U}(\mathbf{X}))} + \sum_{\mathbf{X} \in \Pi_{a,k}^{\text{FD}} \cap \mathcal{A}} \left( R_a \mathbb{1}_{\mathcal{T}_k^{\text{FD}}(\mathbf{X}, \mathcal{U}(\mathbf{X}))} + R_u \mathbb{1}_{\mathcal{T}_k^{\text{FD}}(\mathcal{U}(\mathbf{X}), \mathbf{X})} \right) \right] \right\} \quad (26)$$

where  $\mathcal{A}$  is a bounded space with area  $|\mathcal{A}|$ ,  $\mathcal{U}(\mathbf{x})$  is the associating user to an AP at  $\mathbf{x}$ , and

$$\mathbb{1}_{\mathcal{T}}(\mathbf{x}, \mathbf{y}) \triangleq \begin{cases} 1, & \text{if } (\mathbf{x}, \mathbf{y}) \in \mathcal{T} \\ 0, & \text{otherwise.} \end{cases} \quad (27)$$

Here,  $\mathcal{T}_k^m$  is a random set of transmitter-receiver pairs  $(\mathbf{x}, \mathbf{y})$  that a transmitter at  $\mathbf{x}$  and its corresponding receiver at  $\mathbf{y}$  communicates successfully with higher received SIR than a threshold value  $\tau$ , i.e.,  $(\mathbf{x}, \mathbf{y}) \in \mathcal{T}_k^m$  when

$$\mathcal{T}_k^m = \{(\mathbf{x}, \mathbf{y}) \in \mathbb{R}^d : \gamma_k^m \geq \tau\}.$$

The HDHN throughput measures the average data rate achieved by nodes (e.g., APs and users) communicating successfully in the network, and its unit is bits/sec/Hz/m<sup>2</sup>. One can also define the *cell HDHN throughput* by normalizing the total HDHN throughput achieved over the network,  $|\mathcal{A}| \mathcal{S}$ , with respect to the average number of cells in HDHNs,  $\sum_{i \in \mathcal{K}} |\mathcal{A}| \lambda_i$ , as

$$\mathcal{S}^c = \frac{\mathcal{S}}{\sum_{i \in \mathcal{K}} \lambda_i}. \quad (28)$$

This shows the average data rate per cell in this network and its unit is bits/sec/Hz/cell. Now, we derive the HDHN throughput.

*Lemma 2:* The HDHN throughput is given by

$$\mathcal{S} = \frac{1}{W} \sum_{k=1}^K \lambda_k \left\{ (1 - p_k^{\text{FD}}) R_a p_{S,k}^{\text{HD}}(P_{a,k}, 0, \tau_a) + p_k^{\text{FD}} \left[ R_a p_{S,k}^{\text{FD}}(P_{a,k}, P_{u,k}, \tau_a) + R_u p_{S,k}^{\text{FD}}(P_{u,k}, P_{a,k}, \tau_u) \right] \right\} \quad (29)$$

where  $p_{S,k}^m(P_t, P_r, \tau)$  is defined in (15).

*Proof:* The HDHN throughput in (26) can be represented as

$$\mathcal{S} = \frac{1}{W} \sum_{k=1}^K \lambda_k \left\{ (1 - p_k^{\text{FD}}) R_a \mathbb{E} \left\{ \mathbb{1}_{\mathcal{T}_k^{\text{HD}}(\mathbf{x}, \mathbf{y})} \right\} + p_k^{\text{FD}} \left[ R_a \mathbb{E} \left\{ \mathbb{1}_{\mathcal{T}_k^{\text{FD}}(\mathbf{x}, \mathbf{y})} \right\} + R_u \mathbb{E} \left\{ \mathbb{1}_{\mathcal{T}_k^{\text{FD}}(\mathbf{y}, \mathbf{x})} \right\} \right] \right\}$$

by Campbell's theorem and the stationarity of a homogeneous PPP [60]. Since  $\mathbb{E} \left\{ \mathbb{1}_{\mathcal{T}_k^m(\mathbf{x}, \mathbf{y})} \right\} = p_{S,k}^m(P_t, P_r, \tau)$ , we obtain (29).  $\blacksquare$

We present the HDHN throughput in closed-forms for special cases.

*Corollary 3:* For  $\alpha_i = \alpha > 2$ ,  $\forall i \in \mathcal{K}$  and the perfect self-IC, i.e.,  $C_k^{\text{FD}}(P_r) = 0$ , the HDHN throughput is given by

$$\mathcal{S} = \sum_{k=1}^K \mathcal{S}_k \quad (30)$$

where  $\mathcal{S}_k$  is the throughput of the  $k$ th-tier network, given by

$$\mathcal{S}_k = \frac{1}{2W} \lambda_k \left( \sum_{t \in \mathcal{K}} \lambda_t \mathcal{B}_{tk}^{2/\alpha} \right) \times \left\{ \frac{R_a}{\sum_{i \in \mathcal{K}} \lambda_i \zeta_{ik}(\alpha, P_{a,k})} + \frac{R_u p_k^{\text{FD}}}{\sum_{i \in \mathcal{K}} \lambda_i \zeta_{ik}(\alpha, P_{u,k})} \right\}.$$

*Proof:* It is obtained by substituting (23) into (29).  $\blacksquare$

*Corollary 4:* For  $\alpha_i = 4$ ,  $\forall i \in \mathcal{K}$ , the  $K$ -tier HDHN throughput is given by (31) (on top of the next page).

*Proof:* It is obtained by substituting (20) and (25) into (29).  $\blacksquare$

From Lemma 2, we can see that the HDHN throughput consists of the densities of HD-mode APs, FD-mode APs, and the FD-mode users, and their corresponding successful transmission probabilities. As  $p_k^{\text{FD}}$  increases, there exists more transmitting nodes (e.g., FD-mode users) in the network, but the network interference also increases, which consequently decreases successful transmission probabilities. Hence, it is

$$\begin{aligned}
 S = & \frac{1}{W} \sum_{k=1}^K \lambda_k \sum_{t \in \mathcal{K}} \lambda_t \mathcal{B}_{tk}^{1/2} \left\{ \frac{R_a (1 - p_k^{\text{FD}})}{2 \sum_{i \in \mathcal{K}} \lambda_i \zeta_{ik}(4, P_{a,k})} + \frac{\pi^{3/2} p_k^{\text{FD}}}{2} \right. \\
 & \times \left[ \frac{R_a \sqrt{P_{a,k}}}{\sqrt{\mathcal{C}_k^{\text{FD}}(P_{u,k}) \tau_a}} \exp \left\{ \left( \frac{\sqrt{P_{a,k}} \pi \sum_{i \in \mathcal{K}} \lambda_i \zeta_{ik}(4, P_{a,k})}{\sqrt{\mathcal{C}_k^{\text{FD}}(P_{u,k}) \tau_a}} \right)^2 \right\} \text{Erfc} \left( \frac{\sqrt{P_{a,k}} \pi \sum_{i \in \mathcal{K}} \lambda_i \zeta_{ik}(4, P_{a,k})}{\sqrt{\mathcal{C}_k^{\text{FD}}(P_{u,k}) \tau_a}} \right) \right. \\
 & \left. \left. + \frac{R_u \sqrt{P_{u,k}}}{\sqrt{\mathcal{C}_k^{\text{FD}}(P_{a,k}) \tau_u}} \exp \left\{ \left( \frac{\sqrt{P_{u,k}} \pi \sum_{i \in \mathcal{K}} \lambda_i \zeta_{ik}(4, P_{u,k})}{\sqrt{\mathcal{C}_k^{\text{FD}}(P_{a,k}) \tau_u}} \right)^2 \right\} \text{Erfc} \left( \frac{\sqrt{P_{u,k}} \pi \sum_{i \in \mathcal{K}} \lambda_i \zeta_{ik}(4, P_{u,k})}{\sqrt{\mathcal{C}_k^{\text{FD}}(P_{a,k}) \tau_u}} \right) \right] \right\}. \quad (31)
 \end{aligned}$$

TABLE II  
PARAMETER VALUES IF NOT OTHERWISE SPECIFIED

Parameters	Values	Parameters	Values
$\alpha_k, \forall k$	4	$\lambda_1, \lambda_2$ [nodes/m <sup>2</sup> ]	$10^{-3}$
$T_s$ [sec]	$10^{-4}$	$R_a$ [bits/sec]	$10^4$
$W$ [Hz]	$10^4$	$R_u$ [bits/sec]	$10^4$
$L_{\text{dB},1}$ [dB]	-40	$L_{\text{dB},2}$ [dB]	-30
$P_{a,1}$ [W]	30	$P_{u,1}$ [W]	3
$P_{a,2}$ [W]	30	$P_{u,2}$ [W]	6
$\mathcal{B}_{ij}, \forall i, j$	1	$p_2^{\text{FD}}$	0 (HD mode)

not clear how to determine the portion of FD-mode cells to maximize the throughput of each tier network. From Corollary 3, we obtain the optimal portion of FD-mode cells,  $\hat{p}_k^{\text{FD}}$ , for the perfect self-IC case as follows.

*Corollary 5:* For  $\alpha_k = \alpha > 2$  with  $R_u = R_a$ , when the self-IC in the FD mode is perfect, i.e.,  $\mathcal{C}_k^{\text{FD}}(P_r) = 0$ , the optimal portion of FD-mode APs in the  $k$ th-tier network that maximizes the throughput of the network is  $\hat{p}_k^{\text{FD}} = 1, \forall k \in \mathcal{K}$ .

*Proof:* See Appendix C. ■

*Remark 1:* Corollary 5 shows that, when the self-IC is perfect, in spite of the degradation of successful transmission probability, having more communicating nodes by operating more cells in FD enhances the network throughput. Therefore, in this network, the network throughput is maximized by operating all APs in FD mode regardless of network parameters such as transmission power or AP spatial density.

#### IV. NUMERICAL RESULTS

In this section, we evaluate the throughput of two tier HDHNs consisted of network 1 and network 2 (except for Fig. 9 that considers three tier network), and present the effect of network parameters on the HDHN throughput. Specifically, we first show the HDHN throughput of network 1 in the presence of interference from network 2 as well as network 1 to explore the environment that FD achieves better throughput compared to HD. We then show how to determine the portions of FD-mode APs in two (or three) networks to maximize the HDHN throughput. Note that we use the self-IC capability of nodes in the  $k$ th-tier network as  $\mathcal{C}_k^{\text{FD}}(P_r) = P_r \cdot 10^{L_{\text{dB},k}/10}$ , where  $L_{\text{dB},k}$  [dB] is the ratio of the residual self-interference after IC to the transmission power at the receiver. Unless oth-

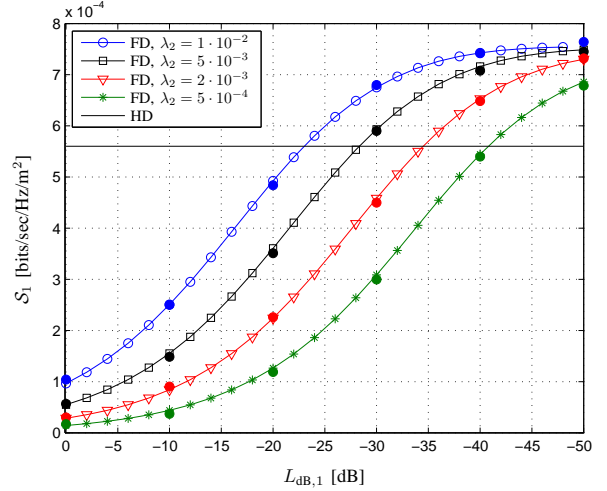


Fig. 3. HDHN throughput of network 1  $S_1$  in bits/sec/Hz/m<sup>2</sup> as a function of the self-IC capability  $L_{\text{dB},1}$  in dB for FD mode ( $p_1^{\text{FD}} = 1$ ) and HD mode ( $p_1^{\text{FD}} = 0$ ) in network 1 and different AP spatial densities of network 2,  $\lambda_2$ , in nodes/m<sup>2</sup> when  $P_{a,1} = 30$  W. Simulation results are marked by filled circles.

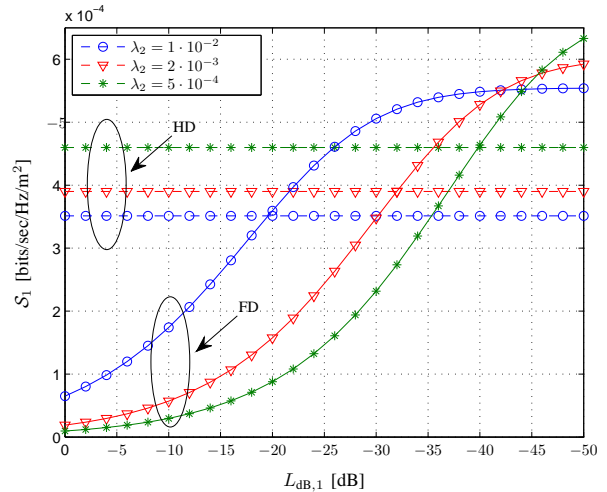


Fig. 4. HDHN throughput of network 1  $S_1$  in bits/sec/Hz/m<sup>2</sup> as a function of the self-IC capability  $L_{\text{dB},1}$  in dB for FD mode ( $p_1^{\text{FD}} = 1$ ) and HD mode ( $p_1^{\text{FD}} = 0$ ) in network 1 and different AP spatial densities of network 2,  $\lambda_2$ , in nodes/m<sup>2</sup> when  $P_{a,1} = 9$  W.

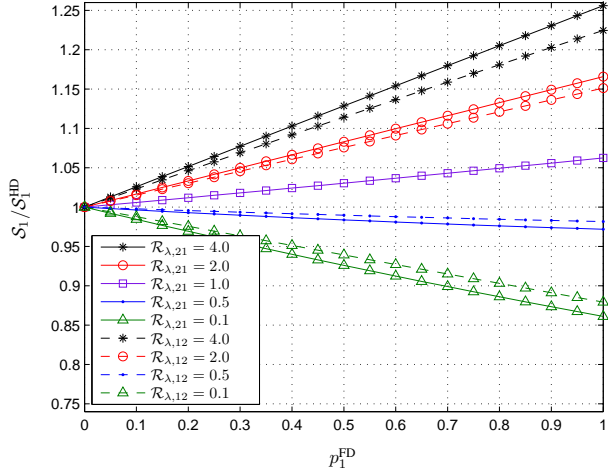


Fig. 5. Ratio of  $S_1$  to the achievable  $S_1$  in HD mode,  $S_1/S_1^{\text{HD}}$ , as a function of  $p_1^{\text{FD}}$  for different duplex modes and different values of  $\mathcal{R}_{\lambda,ij}$ , where  $\mathcal{R}_{\lambda,ij} = \lambda_i/\lambda_j$  for a given  $\lambda_j = 10^{-3}$  nodes/m<sup>2</sup>.

erwise specified, the values of network parameters presented in Table II are used.

Figures 3 and 4 display the HDHN throughput of network 1  $S_1$  as a function of the self-IC capability  $L_{\text{dB},1}$  for different duplex modes in network 1 and different values of AP spatial density of network 2  $\lambda_2$ . Here,  $P_{a,1} = 30$  W is used for Fig. 3 while  $P_{a,1} = 9$  W is used for Fig. 4. Simulation results are marked by filled circles in Fig. 3 and they show a good agreement with the analysis. Note that in Fig. 3,  $S_1$  in HD mode is not changed according to  $\lambda_2$  as  $S_k$  in HD mode is given by

$$S_k = \frac{\lambda_k R_a \mathcal{B}^{2/\alpha}}{2W\zeta(\alpha, P_a)} \quad (32)$$

which is not affected by  $\lambda_i$ ,  $\forall i \neq k$ .<sup>8</sup> However, in Fig. 4,  $S_1$  in HD mode is altered by  $\lambda_2$  as  $P_{a,1} \neq P_{a,2}$ .

From Fig. 3, it can be seen that for large  $\lambda_2$  and low  $L_{\text{dB},1}$ ,  $S_1$  in FD mode is higher than that of HD mode. The effect of low  $L_{\text{dB},1}$  on  $S_1$  is obvious as it means we have smaller residual self-interference. On the other hand, large  $\lambda_2$  affects the network throughput in two aspects: 1) increasing the network interference (negative effect); and 2) making an user associate to closer AP with higher probability (positive effect). As  $\lambda_2$  increases, we have large network interference, which makes the effect of self-interference on  $S_1$  less in FD mode and the successful transmission probabilities in FD and HD modes relatively similar. Hence, for large  $\lambda_2$  or low  $L_{\text{dB},1}$ , operating APs in FD achieves higher  $S_1$  compared to that in HD due to additionally communicating users in FD mode.

<sup>8</sup>Specifically, for  $\alpha_k = \alpha$ ,  $\mathcal{B}_{ik} = \mathcal{B}$ , and  $P_{a,k} = P_a$ ,  $\forall k, i$ , we have  $\sigma_{ik}(\alpha, P_a) = \sigma(\alpha, P_a)$  and  $\zeta_{ik}(\alpha, P_a) = \zeta(\alpha, P_a)$ ,  $\forall k, i$ . Hence, from (25) and (29),  $S_k$  in HD mode is represented by

$$S_k = \frac{R_a}{W} \sum_{k=1}^2 \lambda_k \frac{\mathcal{B}^{2/\alpha} \left( \sum_{k=1}^2 \lambda_k \right)}{2\zeta(\alpha, P_a) \left( \sum_{k=1}^2 \lambda_k \right)} = \frac{\lambda_k R_a \mathcal{B}^{2/\alpha}}{2W\zeta(\alpha, P_a)}.$$

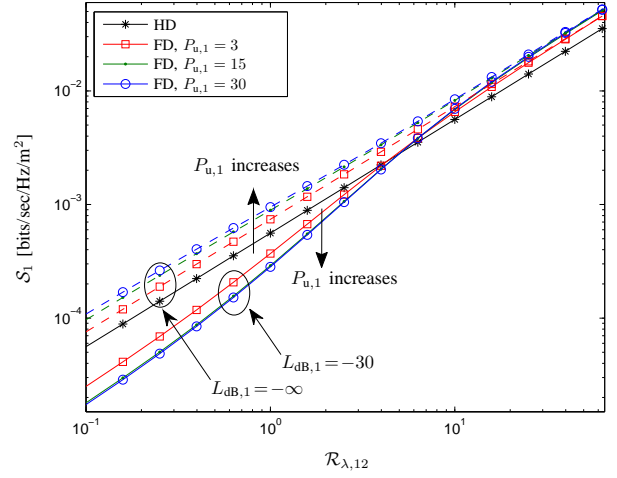


Fig. 6. HDHN throughput of network 1  $S_1$  in bits/sec/Hz/m<sup>2</sup> as a function of  $\mathcal{R}_{\lambda,12}$  with  $\lambda_2 = 10^{-3}$  nodes/m<sup>2</sup> for different values of  $P_{a,1}$  in W and  $L_{\text{dB},1}$  in dB and different duplex modes.

From Fig. 3, we can also see that for a fixed  $L_{\text{dB},1}$ ,  $S_1$  in FD mode increases with  $\lambda_2$ . This is due to the fact that when the self-interference is large, as  $\lambda_2$  increases, the increased network interference affects less than the shorter distance to associated AP. However, this results becomes different when the self-interference is small as shown in Fig. 4. In Fig. 4, we can see that  $S_1$  in FD mode decreases as  $\lambda_2$  increases when  $L_{\text{dB},1} < -45$ . This can be attributed to the fact that for small self-interference,  $S_1$  is changed more by the increased network interference than the shorter communication link distance. Hence, in this case, having smaller  $\lambda_2$  can enhance  $S_1$ . This result is also applied for the HD mode case. From Fig. 4, we can see that  $S_1$  in HD mode decreases as  $\lambda_2$  increases due to the large effect of the increased network interference.

Figure 5 shows the ratio of  $S_1$  to the achievable  $S_1$  when  $p_1^{\text{FD}} = 0$  (i.e., when all APs are operating in HD mode),  $S_1^{\text{FD}}$ , as a function of the FD-mode AP portion  $p_1^{\text{FD}}$  for different values of AP spatial density ratios  $\mathcal{R}_{\lambda,12}$  and  $\mathcal{R}_{\lambda,21}$  when  $\lambda_i$  is varied as  $\lambda_i = \mathcal{R}_{\lambda,ij} \lambda_j$  for a given  $\lambda_j = 10^{-3}$ . This figure shows how much  $S_1$  increases or decreases in FD compared to achievable  $S_1$  in HD. Furthermore, larger  $\mathcal{R}_{\lambda,12}$  or  $\mathcal{R}_{\lambda,21}$  means larger  $\lambda_i$  where  $\lambda_i = \lambda_1 + \lambda_2$ , and  $\lambda_i = (1 + \mathcal{R}_{\lambda,ij}) \cdot 10^{-3}$  in this figure. From Fig. 5, it can be seen that  $S_1$  increases with  $p_1^{\text{FD}}$  for high  $\lambda_i$  while it decreases for low  $\lambda_i$ . This can be attributed to the fact that the FD mode achieves higher throughput than the HD mode for large  $\lambda_i$  as also shown in Fig. 3. In Fig. 5,  $S_1^{\text{FD}}$  either increases or decreases with  $p_1^{\text{FD}}$  over all range of  $p_1^{\text{FD}}$ . This shows, in terms of the throughput of a tier network, operating all APs either in FD mode or HD mode achieves the maximum throughput compared to the mixture of two mode APs. For example, when  $\mathcal{R}_{\lambda,ij}$  is greater than 1 in Fig. 5, deploying FD-mode APs in all cells of network 1 achieves the maximum  $S_1$ .

Figure 6 displays  $S_1$  as a function of  $\mathcal{R}_{\lambda,12}$  with  $\lambda_2 = 10^{-3}$  for different values of  $P_{a,1}$  and  $L_{\text{dB},1}$  and different duplex modes. Note that  $S_1$  increases with  $\lambda_1$  as shown in (32).



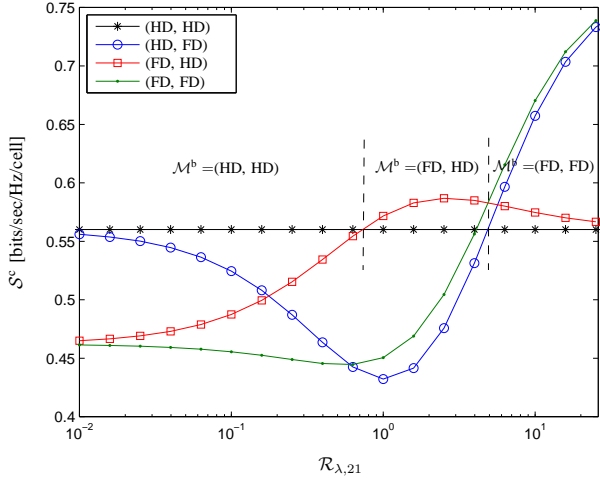


Fig. 7. Cell HDHN throughput  $S^c$  in bits/sec/Hz/cell as a function of  $\mathcal{R}_{\lambda,21}$  with  $\lambda_1 = 10^{-3}$  nodes/m<sup>2</sup> for different sets  $(m_1, m_2)$  of duplex modes in network 1  $m_1$  and network 2  $m_2$ .

From Fig. 6, it can be seen that for  $\mathcal{R}_{\lambda,12} < 4$ , the HD mode achieves higher  $\mathcal{S}_1$  than the FD mode when  $L_{dB,1} = -30$ , but it becomes opposite for the perfect self-IC, i.e.,  $L_{dB,1} = -\infty$ . This is also verified in Corollary 5, which shows the optimal portion of FD-mode APs is  $\hat{p}_k^{FD} = 1, \forall k$ , for  $\mathcal{C}_k^{FD}(P_r) = 0$ . From Fig. 6, it can be also seen that, for  $\mathcal{R}_{\lambda,12} < 4$ ,  $\mathcal{S}_1$  in FD mode increases as  $P_{u,1}$  increases for  $L_{dB,1} = -\infty$  while it decreases for  $L_{dB,1} = -30$ . This is due to the fact that, for high self-IC capability, the network throughput in FD mode increases with  $P_{u,1}$  since higher  $P_{u,1}$  provides more reliable communication between a user and its associated AP. On the other hand, for low self-IC capability, the self-interference mainly determines the network throughput, so lower  $P_{u,1}$  achieves higher  $\mathcal{S}_1$ . From Fig. 6, we can also see that the  $\mathcal{S}_1$  in FD mode with  $L_{dB,1} = -30$  converges to that with  $L_{dB,1} = -\infty$  as  $\lambda_1$  increases. This is due to the fact that as we have large network interference (i.e., large  $\lambda_1$ ), the network interference mainly determines the network throughput while the effect of residual self-interference becomes marginal. Due to the relatively weak effect of self-interference for large  $\lambda_1$ , when  $\mathcal{R}_{\lambda,12} > 4$ ,  $\mathcal{S}_1$  in FD mode with  $L_{dB,1} = -30$  becomes larger than  $\mathcal{S}_1$  in HD mode as we have additional communicating users in FD mode.

Now, we present the HDHN throughput for two networks. Figure 7 shows the cell HDHN throughput  $S^c$  as a function of  $\mathcal{R}_{\lambda,21}$  with  $\lambda_1 = 10^{-3}$  for different duplex mode set  $(m_1, m_2)$ , where  $m_i$  is the duplex mode of network  $i$ ,  $\forall i \in \{1, 2\}$ . Here,  $\mathcal{M}^b$  is the best duplex mode set  $(m_1, m_2)$  that achieves the highest  $S^c$ . Note that due to the network parameters used for this figure, from (28) and (32),  $S^c$  in (HD, HD) is presented by

$$S^c = \frac{R_a \mathcal{B}^{2/\alpha}}{2W\zeta(\alpha, P_a)}$$

which is not affected by any  $\lambda_i, \forall i$  (nor by  $\mathcal{R}_{\lambda,ij}$ ). Note also that, for a given  $\mathcal{R}_{\lambda,ij}$ , the best duplex mode set in terms of  $S^c$  is equal to that in terms of  $\mathcal{S}$  as  $\mathcal{S}$  is the scaling of  $S^c$  with

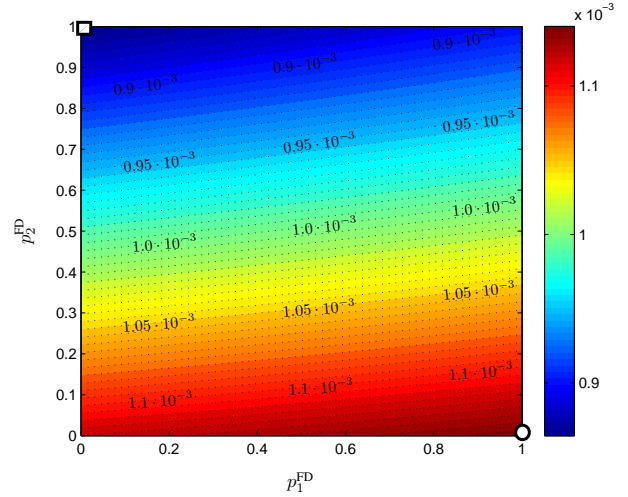


Fig. 8. HDHN throughput  $\mathcal{S}$  in bits/sec/Hz/m<sup>2</sup> as a function of  $p_1^{FD}$  and  $p_2^{FD}$  (the square and the circle are the points achieving the minimum and the maximum  $\mathcal{S}$ , respectively).

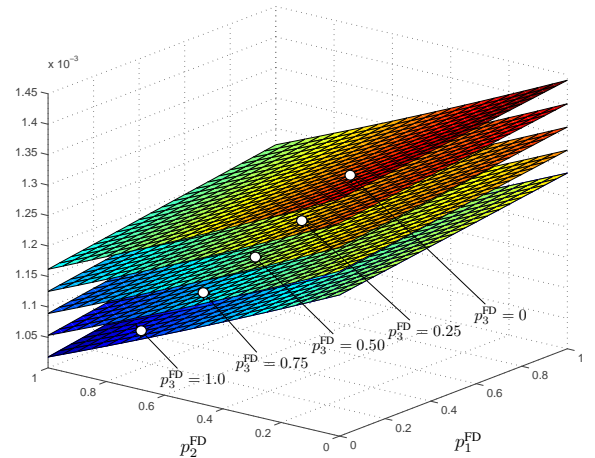


Fig. 9. HDHN throughput  $\mathcal{S}$  in bits/sec/Hz/m<sup>2</sup> of three tier networks as a function of  $p_1^{FD}$ ,  $p_2^{FD}$ , and  $p_3^{FD}$ . For network 3,  $\lambda_3 = 5 \cdot 10^{-4}$  nodes/m<sup>2</sup>,  $P_{a,3} = 15$  W,  $P_{u,3} = 3$  W, and  $L_{dB,3} = -20$  dB are used.

$\lambda_i$ . From Fig. 7, it can be seen that the best duplex mode set is (FD, FD) for large  $\mathcal{R}_{\lambda,21}$  because the FD mode achieves better throughput than the HD mode for large  $\lambda_i$ . It can be also seen that the  $\mathcal{R}_{\lambda,21}$  value that changes the best duplex mode from HD to FD in the network 1 is generally smaller than that in the network 2. This can be attributed to the fact that the network 1 has better self-IC capability and lower  $P_{u,1}$ , so the self-interference in the network 1 is smaller than that in the network 2. Hence, the FD mode is preferred to HD mode even for small  $\lambda_2$  in the network 1. From this figure, it can be seen that the hybrid-duplex mode set can enhance the throughput of heterogeneous network for the  $\mathcal{R}_{\lambda,21}$  range of  $\mathcal{M}^b = (\text{FD}, \text{HD})$ . This is also verified in the following figure.

Figure 8 displays the contour of  $\mathcal{S}$  as a function of  $p_1^{FD}$  and  $p_2^{FD}$ . It can be seen that  $\mathcal{S}$  is maximized when  $p_1^{FD} = 1$

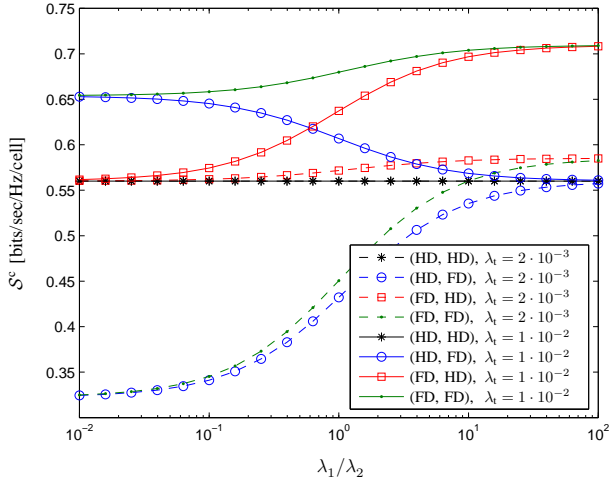


Fig. 10. Cell HDHN throughput  $\mathcal{S}^c$  in bits/sec/Hz/cell as a function of the ratio  $\lambda_1/\lambda_2$  for different values of  $\lambda_t = \lambda_1 + \lambda_2$  in nodes/m<sup>2</sup> and different duplex mode set  $(m_1, m_2)$ .

and  $p_2^{\text{FD}} = 0$  (the point marked by a circle in the figure), i.e., (FD, HD), which is the same result for  $\mathcal{R}_{\lambda,21} = 1$  in Fig. 7. Hence, by operating APs of network 1 in FD mode and APs of network 2 in HD mode, we achieve the maximum HDHN throughput. From Fig. 8, it can be also seen that  $\mathcal{S}$  keeps increasing with  $p_1^{\text{FD}}$  and decreasing with  $p_2^{\text{FD}}$ . This also verifies that, within a tier network, operating all APs either in FD or HD achieves higher  $\mathcal{S}$  compared to having APs in both modes. This can be also verified in Fig. 9, which displays the HDHN throughput  $\mathcal{S}$  for three tier networks as a function of  $p_1^{\text{FD}}$  and  $p_2^{\text{FD}}$  for different values of  $p_3^{\text{FD}}$ . From this figure, we can see that the maximum  $\mathcal{S}$  can be achieved by operating all APs in network 1, 2, and network 2 in HD ( $p_1^{\text{FD}} = 0$ ), FD ( $p_2^{\text{FD}} = 1$ ), and HD ( $p_3^{\text{FD}} = 0$ ) modes, respectively.

Figure 10 shows the cell HDHN throughput  $\mathcal{S}^c$  for two tier network as a function of the ratio  $\lambda_1/\lambda_2$  for different values of  $\lambda_t = \lambda_1 + \lambda_2$  and different duplex mode set  $(m_1, m_2)$ . From Fig. 10, it can be seen that the best duplex mode sets for  $\lambda_t = 2 \cdot 10^{-3}$  and  $\lambda_t = 1 \cdot 10^{-2}$  are (FD, HD) and (FD, FD), respectively, for all the range of  $\lambda_1/\lambda_2$ . Hence, we can see that the best duplex mode is determined more by the total density of APs in HDHNs  $\lambda_t$  than the AP density ratio,  $\lambda_1/\lambda_2$ .

## V. CONCLUSION

This paper establishes a foundation for HDHNs accounting for the spatial AP distribution, the self-IC capability, and the network interference. After newly characterizing the network interference generated by FD-mode cells, we define and derive the HDHN throughput. By quantifying the HDHN throughput, we show the effect of network parameters and self-IC capabilities on the HDHN throughput, and present how to optimally determine the duplex mode to maximize the HDHN throughput. Specifically, our results demonstrate that the FD mode achieves higher network throughput than the HD mode for high self-IC capability and large AP density of HDHNs. In order to maximize the throughput of a tier network, operating

all APs in either HD or FD is better than having two mode APs. On the other hand, in terms of the total throughput of heterogeneous networks, making different tier networks operate in different duplex modes can enhance the throughput. The outcomes of our work provide insights on the efficient design of HDHNs, and opens several issues for future research on HDHNs including the transmission power control for FD- and HD-mode nodes, the throughput of MIMO FD system in the presence of network interference, the effect of network interference cancellation on the HDHN throughput, and the communication secrecy of HDHNs.

## APPENDIX

### A. Proof of Lemma 1

The Laplace transform  $\mathcal{L}_{I_i^{\text{FD}}}(s)$  is given by

$$\begin{aligned} \mathcal{L}_{I_i^{\text{FD}}}(s) & \stackrel{(a)}{=} \exp \left\{ -2\pi\lambda_i^{\text{FD}} \int_{\hat{D}} x \mathbb{E}_{G_i} \left\{ 1 - e^{-sG_i x^{-\alpha_i}} \right\} dx \right\} \\ & = \exp \left\{ -2\pi\lambda_i^{\text{FD}} \mathbb{E}_{G_i} \left\{ \int_{\hat{D}} x \left( 1 - e^{-sG_i x^{-\alpha_i}} \right) dx \right\} \right\} \\ & \stackrel{(b)}{=} \exp \left\{ -\frac{2}{\alpha_i} \pi\lambda_i^{\text{FD}} \mathbb{E}_{G_i} \left\{ \int_{\hat{D}^{\alpha_i}} y^{2/\alpha_i-1} \left( 1 - e^{-sG_i/y} \right) dy \right\} \right\} \end{aligned} \quad (33)$$

where (a) is from the Campbell's theorem [60],<sup>9</sup> and (b) is obtained by replacing  $y$  for  $x^{\alpha_i}$ . In (33), by replacing  $z$  for  $1/y$ , the integral inside of the expectation is represented as

$$\begin{aligned} & \int_{\hat{D}^{\alpha_i}} y^{2/\alpha_i-1} \left( 1 - e^{-sG_i/y} \right) dy \\ & = \int_0^{\frac{1}{\hat{D}^{\alpha_i}}} z^{-2/\alpha_i-1} \left( 1 - e^{-sG_i z} \right) dz \\ & = \int_0^{\infty} z^{-\frac{2}{\alpha_i}-1} \left( 1 - e^{-sG_i z} \right) dz - \int_{\frac{1}{\hat{D}^{\alpha_i}}}^{\infty} z^{-\frac{2}{\alpha_i}-1} dz \\ & \quad + \int_{\frac{1}{\hat{D}^{\alpha_i}}}^{\infty} z^{-\frac{2}{\alpha_i}-1} e^{-sG_i z} dz. \end{aligned} \quad (34)$$

In (34), from [59, eq. (3.478)] and [59, eq. (3.381)], the first and the third integrals are respectively given by

$$\begin{aligned} & \int_0^{\infty} z^{-\frac{2}{\alpha_i}-1} \left( 1 - e^{-sG_i z} \right) dz = - (sG_i)^{\frac{2}{\alpha_i}} \Gamma \left( -\frac{2}{\alpha_i} \right), \quad \forall \alpha_i > 2 \\ & \int_{\frac{1}{\hat{D}^{\alpha_i}}}^{\infty} z^{-\frac{2}{\alpha_i}-1} e^{-sG_i z} dz = (sG_i)^{\frac{2}{\alpha_i}} \Gamma \left( -\frac{2}{\alpha_i}, \frac{sG_i}{\hat{D}^{\alpha_i}} \right). \end{aligned} \quad (35)$$

Therefore, by using (34) in (33) after representing it using  $\Gamma \left( -\frac{2}{\alpha_i} \right) = \frac{-\alpha_i}{2} \Gamma \left( 1 - \frac{2}{\alpha_i} \right)$ ,  $\int_{\frac{1}{\hat{D}^{\alpha_i}}}^{\infty} z^{-\frac{2}{\alpha_i}-1} dz = \frac{\alpha_i \hat{D}^2}{2}$ , and

<sup>9</sup>For a homogeneous PPP  $\Pi_o \in \mathbb{R}^d$  with density  $\lambda_o$ , the Campbell's theorem shows the following property holds [60]

$$\mathbb{E}_{\Pi_o} \left\{ \sum_{\mathbf{Y} \in \Pi_o \cup \mathcal{A}} g(\mathbf{Y}) \right\} = \lambda_o \int_{\mathcal{A}} g(\mathbf{y}) d\mathbf{y}$$

where  $\mathcal{A}$  is a bounded space and  $g(\mathbf{y})$  is a bounded measurable function for  $\mathbf{y} \in \mathbb{R}^d$ .

(35), we can obtain  $\mathcal{L}_{I_i^{\text{FD}}}(s)$  as

$$\begin{aligned} & \mathcal{L}_{I_i^{\text{FD}}}(s) \\ &= \exp \left\{ -\pi \lambda_i^{\text{FD}} \left[ -\hat{D}^2 + s^{2/\alpha_i} \mathbb{E}_{G_i} \left\{ G_i^{2/\alpha_i} \right\} \Gamma \left( 1 - \frac{2}{\alpha_i} \right) \right. \right. \\ & \quad \left. \left. + \frac{2}{\alpha_i} s^{2/\alpha_i} \mathbb{E}_{G_i} \left\{ G_i^{2/\alpha_i} \Gamma \left( -\frac{2}{\alpha_i}, \frac{s G_i}{\hat{D}^{\alpha_i}} \right) \right\} \right] \right\} \quad (36) \end{aligned}$$

for  $\alpha_i > 2$ .

From (11), for  $P_{a,i} \neq P_{u,i}$ ,  $\forall i \in \mathcal{K}$ , we have

$$\begin{aligned} & \mathbb{E}_{G_i} \left\{ G_i^{2/\alpha_i} \Gamma \left( -\frac{2}{\alpha_i}, \frac{s G_i}{\hat{D}^{\alpha_i}} \right) \right\} \\ &= \frac{1}{P_{u,i} - P_{a,i}} \int_0^\infty g^{2/\alpha_i} \Gamma \left( -\frac{2}{\alpha_i}, \frac{g s}{\hat{D}^{\alpha_i}} \right) \left( e^{-\frac{g}{P_{u,i}}} - e^{-\frac{g}{P_{a,i}}} \right) dg \\ &\stackrel{(a)}{=} \frac{1}{P_{u,i} - P_{a,i}} \left\{ \mathcal{I}_1 \left( \frac{2}{\alpha_i} + 1, \frac{1}{P_{u,i}}, \frac{-2}{\alpha_i}, \frac{s}{\hat{D}^{\alpha_i}} \right) \right. \\ & \quad \left. - \mathcal{I}_1 \left( \frac{2}{\alpha_i} + 1, \frac{1}{P_{a,i}}, \frac{-2}{\alpha_i}, \frac{s}{\hat{D}^{\alpha_i}} \right) \right\} \quad (37) \end{aligned}$$

where  $\mathcal{I}_1(x, y, z, \nu)$  is defined in (14) and (a) is obtained by [59, eq. 6.455]. For  $P_{a,i} = P_{u,i}$ , we have

$$\begin{aligned} & \mathbb{E}_{G_i} \left\{ G_i^{2/\alpha_i} \Gamma \left( -\frac{2}{\alpha_i}, \frac{s G_i}{\hat{D}^{\alpha_i}} \right) \right\} \\ &= \frac{1}{P_{a,i}^2} \int_0^\infty g^{2/\alpha_i + 1} \Gamma \left( -\frac{2}{\alpha_i}, \frac{g s}{\hat{D}^{\alpha_i}} \right) e^{-g/P_{a,i}} dg \\ &= \frac{1}{P_{a,i}^2} \mathcal{I}_1 \left( \frac{2}{\alpha_i} + 2, \frac{1}{P_{a,i}}, \frac{-2}{\alpha_i}, \frac{s}{\hat{D}^{\alpha_i}} \right). \quad (38) \end{aligned}$$

Using (11), we can readily obtain  $\mathbb{E}_{G_i} \left\{ G_i^{2/\alpha_i} \right\}$  in (36). Finally, by substituting (11), (37), and (38) into (36), we obtain (13).

### B. Proof of Theorem 1

The complementary cumulative distribution function (CCDF) of SIR in (5) is presented for Rayleigh fading channels as

$$\begin{aligned} & \mathbb{P} \{ \gamma_k^m \geq \tau \} \\ &= \mathbb{E} \left\{ \exp \left\{ -\frac{D^{\alpha_k} \tau}{P_t} \left( C_k^m(P_r) + \sum_{i \in \mathcal{K}} (I_i^{\text{HD}} + I_i^{\text{FD}}) \right) \right\} \right\} \\ &= \mathbb{E}_D \left\{ e^{-\frac{D^{\alpha_k} \tau C_k^m(P_r)}{P_t}} \prod_{i \in \mathcal{K}} \mathcal{L}_{I_i^{\text{HD}}} \left( \frac{D^{\alpha_k} \tau}{P_t} \right) \mathcal{L}_{I_i^{\text{FD}}} \left( \frac{D^{\alpha_k} \tau}{P_t} \right) \right\} \quad (39) \end{aligned}$$

where  $D$  is the distance from a typical user to its associated AP and  $\mathcal{L}_Z(s) = \mathbb{E}_Z \{ e^{-sZ} \}$  is the Laplace transform of  $Z$ . Using the PDF of  $D$  in (3), we can represent (39) as

$$\begin{aligned} & \mathbb{P} \{ \gamma_k^m > \tau \} = \frac{2\pi \lambda_k^m}{P_{A,k}} \int_0^\infty r e^{-\frac{C_k^m(P_r) \tau}{P_t} r^{\alpha_k} - \pi \sum_{i \in \mathcal{K}} \lambda_i \mathcal{B}_{ik}^{\frac{\alpha_i}{\alpha_k}} r^{\frac{2\alpha_k}{\alpha_i}}} \\ & \quad \times \prod_{i \in \mathcal{K}} \mathcal{L}_{I_i^{\text{HD}}} \left( \frac{r^{\alpha_k} \tau}{P_t} \right) \mathcal{L}_{I_i^{\text{FD}}} \left( \frac{r^{\alpha_k} \tau}{P_t} \right) dr. \quad (40) \end{aligned}$$

In (40),  $\mathcal{L}_{I_i^{\text{HD}}}(s)$ ,  $\forall s > 0$  can be represented by

$$\begin{aligned} & \mathcal{L}_{I_i^{\text{HD}}}(s) \stackrel{(a)}{=} \exp \left\{ -2\pi \lambda_i^{\text{HD}} \int_{\hat{D}}^\infty x \mathbb{E}_H \left\{ 1 - e^{-s P_{a,i} H x^{\alpha_i}} \right\} dx \right\} \\ &= \exp \left\{ -2\pi \lambda_i^{\text{HD}} \int_{\hat{D}}^\infty \frac{x}{1 + (s^{-1} P_{a,i}^{-1} x^{\alpha_i})} dx \right\} \quad (41) \end{aligned}$$

where  $\hat{D}$  is the distance to nearest unassociated AP, given by [43]

$$\hat{D} = \mathcal{B}_{ik}^{1/\alpha_i} D^{\alpha_k/\alpha_i}. \quad (42)$$

In (41), (a) is from the Campbell's theorem [60] and the integral over  $x$  is performed from  $\hat{D}$  since, due to the association rule,  $\mathcal{W}_k D_k^{-\alpha_k}$  is the minimum value among  $\mathcal{W}_i D_i^{-\alpha_i}$ ,  $\forall i \in \mathcal{K}$ , where  $D_i$  is the distance between a typical user to the nearest AP in the  $i$ th-tier network. By replacing  $s = r^{\alpha_k} \tau P_t^{-1}$  and  $\hat{D} = \mathcal{B}_{ik}^{1/\alpha_i} r^{\alpha_k/\alpha_i}$  in (41), we have

$$\begin{aligned} & \mathcal{L}_{I_i^{\text{HD}}} \left( \frac{r^{\alpha_k} \tau}{P_t} \right) \\ &= \exp \left\{ -2\pi \lambda_i^{\text{HD}} \int_{\mathcal{B}_{ik}^{1/\alpha_i} r^{\alpha_k/\alpha_i}}^\infty \frac{x}{1 + P_t (r^{\alpha_k} \tau P_{a,i})^{-1} x^{\alpha_i}} dx \right\} \\ &= \exp \left\{ -2\pi \lambda_i (1 - p_i^{\text{FD}}) r^{2\alpha_k/\alpha_i} \mathcal{I}_0 \left( r^{\alpha_k}, \frac{P_t}{\tau P_{a,i}}, \mathcal{B}_{ik}, \alpha_i \right) \right\} \end{aligned}$$

where  $\mathcal{I}_0(x, y, z, \nu)$  is defined in (19) using [59, eq. (3.194)]. From (19), we can see that the parameter  $x$  does not affect  $\mathcal{I}_0(x, y, z, \nu)$ . Hence, we have  $\mathcal{I}_0(x, y, z, \nu) = \mathcal{I}_0(1, y, z, \nu)$  and

$$\begin{aligned} & \prod_{i \in \mathcal{K}} \mathcal{L}_{I_i^{\text{HD}}} \left( \frac{r^{\alpha_k} \tau}{P_t} \right) = \exp \left\{ -2\pi \sum_{i \in \mathcal{K}} \lambda_i (1 - p_i^{\text{FD}}) r^{2\alpha_k/\alpha_i} \right. \\ & \quad \left. \times \mathcal{I}_0 \left( 1, \frac{P_t}{\tau P_{a,i}}, \mathcal{B}_{ik}, \alpha_i \right) \right\}. \quad (43) \end{aligned}$$

In Lemma 1, by replacing  $s = r^{\alpha_k}/P_t$  and  $\hat{D} = \mathcal{B}_{ik}^{1/\alpha_i} r^{\alpha_k/\alpha_i}$ , we have<sup>10</sup>

$$\begin{aligned} & \prod_{i \in \mathcal{K}} \mathcal{L}_{I_i^{\text{FD}}} \left( \frac{r^{\alpha_k} \tau}{P_t} \right) = \exp \left\{ -2\pi \sum_{i \in \mathcal{K}} \lambda_i p_i^{\text{FD}} r^{2\alpha_k/\alpha_i} \right. \\ & \quad \times \left[ -\frac{1}{2} \mathcal{B}_{ik}^{2/\alpha_i} + \frac{\tau^{2/\alpha_i}}{2 P_t^{2/\alpha_i}} \Gamma \left( 1 - \frac{2}{\alpha_i} \right) \mathbb{E}_{G_i} \left\{ G_i^{2/\alpha_i} \right\} \right. \\ & \quad \left. \left. + \frac{\tau^{2/\alpha_i}}{\alpha_i P_t^{2/\alpha_i}} \mathbb{E}_{G_i} \left\{ G_i^{2/\alpha_i} \Gamma \left( -\frac{2}{\alpha_i}, \frac{G_i \tau}{P_t \mathcal{B}_{ik}} \right) \right\} \right] \right\}. \quad (44) \end{aligned}$$

Finally, substituting (2), (43) and (44) into (40) results in (15).

<sup>10</sup>The (44) is obtained when the biased distance to the associated AP from a typical user  $\mathcal{W}_k D_k^{-\alpha_k}$  is smaller than that to any APs. In FD-mode cells, the biased distance from the typical user to a user, who associates to another AP, can be smaller than that to the associated AP. However, we ignore this case since a user generally transmits with smaller power than an AP and for analytical tractability.

### C. Proof of Corollary 5

When  $R_u = R_a = R_t$ , the throughput of  $k$ th-tier network  $S_k$  in (30) is represented by

$$S_k = \frac{R_t}{2W} \lambda_k \left( \sum_{t \in \mathcal{K}} \lambda_t \mathcal{B}_{tk}^{2/\alpha} \right) S_k^o \quad (45)$$

where  $S_k^o$  is given by

$$S_k^o = \frac{1}{\sum_{i \in \mathcal{K}} \lambda_i \zeta_{ik}(\alpha, P_{a,k})} + \frac{p_k^{\text{FD}}}{\sum_{i \in \mathcal{K}} \lambda_i \zeta_{ik}(\alpha, P_{u,k})} \quad (46)$$

From (16),  $\zeta_{ik}(\alpha, P_t)$  in (46) can be represented by

$$\zeta_{ik}(\alpha, P_t) = \delta_{ik}(P_t) p_i^{\text{FD}} + \tilde{\delta}_{ik}(P_t) \quad (47)$$

where  $\delta_{ik}(P_t)$  and  $\tilde{\delta}_{ik}(P_t)$  are given by

$$\begin{aligned} \delta_{ik}(P_t) &= \tilde{\sigma}_{ik}(\alpha, P_t) - \sigma_{ik}(\alpha, P_t) \\ \tilde{\delta}_{ik}(P_t) &= \sigma_{ik}(\alpha, P_t) + \frac{\mathcal{B}_{ik}^{2/\alpha}}{2}. \end{aligned}$$

Here, for the equal density  $\lambda_o$  of FD-mode and HD-mode APs,  $\mathcal{L}_{I_i^{\text{HD}}}(s)^2 \leq \mathcal{L}_{I_i^{\text{FD}}}(s) \leq \mathcal{L}_{I_i^{\text{HD}}}(s)$ .<sup>11</sup> Since  $\mathcal{L}_{I_i^{\text{HD}}}\left(\frac{r^\alpha \tau}{P_t}\right) = \exp\{-2\pi\lambda_o r^2 \sigma_{ik}(\alpha, P_t)\}$  and  $\mathcal{L}_{I_i^{\text{FD}}}\left(\frac{r^\alpha \tau}{P_t}\right) = \exp\{-2\pi\lambda_o r^2 \tilde{\sigma}_{ik}(\alpha, P_t)\}$ , we have

$$\sigma_{ik}(\alpha, P_t) \leq \tilde{\sigma}_{ik}(\alpha, P_t) \leq 2\sigma_{ik}(\alpha, P_t).$$

Hence,  $\delta_{ik}(P_t) > 0$  and

$$\delta_{ik}(P_t) \leq \tilde{\delta}_{ik}(P_t). \quad (48)$$

In (46),  $\sum_{i \in \mathcal{K}} \lambda_i \zeta_{ik}(\alpha, P_{u,k})$  can be presented as a function of  $p_k^{\text{FD}}$  as

$$\sum_{i \in \mathcal{K}} \lambda_i \zeta_{ik}(\alpha, P_t) = c_1(P_t) p_i^{\text{FD}} + c_2(P_t) \quad (49)$$

where  $c_1(P_t)$  and  $c_2(P_t)$  are given by

$$\begin{aligned} c_1(P_t) &= \lambda_k \delta_{kk}(P_t) \\ c_2(P_t) &= \lambda_k \tilde{\delta}_{kk}(P_t) + \sum_{j \neq k, j \in \mathcal{K}} \lambda_j \zeta_{jk}(\alpha, P_t). \end{aligned}$$

Then, using (49) in (46), we can obtain the first derivative of  $S_k^o$  according to  $p_k^{\text{FD}}$  as

$$\frac{\partial S_k^o}{\partial p_k^{\text{FD}}} = \frac{-c_1(P_{a,k})}{(c_1(P_{a,k}) p_k^{\text{FD}} + c_2(P_{a,k}))^2} + \frac{c_2(P_{u,k})}{(c_1(P_{u,k}) p_k^{\text{FD}} + c_2(P_{u,k}))^2} \quad (50)$$

for all  $i \in \mathcal{K}$ . Here,  $c_1(P_t) \leq c_2(P_t)$  since  $\delta_{ik}(P_t) \leq \tilde{\delta}_{ik}(P_t)$  in (48), and<sup>12</sup>

$$c_1(P_{u,k}) p_k^{\text{FD}} + c_2(P_{u,k}) \geq c_1(P_{a,k}) p_k^{\text{FD}} + c_2(P_{a,k}), \quad \forall k, \forall p_k^{\text{FD}}.$$

Hence,  $c_1(P_t)$  and  $c_2(P_t)$  are decreasing function according to  $P_t$ , and we can see that  $\frac{c_2(P_{u,k})}{(c_1(P_{u,k}) p_k^{\text{FD}} + c_2(P_{u,k}))^2}$  in (50) decreases

<sup>11</sup>For the equal density of APs, from (6) and (7),  $I_i^{\text{FD}}$  is always not less than  $I_i^{\text{HD}}$ , which results in  $\mathcal{L}_{I_i^{\text{FD}}}(s) \leq \mathcal{L}_{I_i^{\text{HD}}}(s)$ . In addition,  $\mathcal{L}_{I_i^{\text{FD}}}(s) = \mathbb{E}_{I_i^{\text{FD}}}\{e^{-s I_i^{\text{FD}}}\} \leq \mathbb{E}_{I_i^{\text{HD}}}\{e^{-s I_i^{\text{HD}}}\}$ , which gives  $\mathcal{L}_{I_i^{\text{HD}}}(s)^2 \leq \mathcal{L}_{I_i^{\text{FD}}}(s)$ .

<sup>12</sup>This relation can be presented using (49) and  $\zeta_{ik}(\alpha, P_{a,k}) \leq \zeta_{ik}(\alpha, P_{u,k})$ , obtained from  $p_{S,k}^{\text{FD}}(P_{a,k}, 0, \tau) \geq p_{S,k}^{\text{FD}}(P_{u,k}, 0, \tau)$  in (23).

as  $P_{u,k}$  decreases (i.e., as both  $c_1(P_{u,k})$  and  $c_2(P_{u,k})$  increases). Here, when  $P_{u,k} = P_{a,k}$ , from (50), we have

$$\frac{\partial S_k^o}{\partial p_k^{\text{FD}}} = \frac{c_2(P_{a,k}) - c_1(P_{a,k})}{(c_1(P_{a,k}) p_k^{\text{FD}} + c_2(P_{a,k}))^2} \geq 0. \quad (51)$$

When  $P_{u,k} = 0$ ,  $p_{S,k}^{\text{FD}}(P_{a,k}, P_{u,k}, \tau) = p_{S,k}^{\text{HD}}(P_{a,k}, 0, \tau)$  and  $p_{S,k}^{\text{FD}}(P_{u,k}, P_{a,k}, \tau) = 0$ , so from (23) and (29), we have

$$S_k^o = \frac{1}{\sum_{i \in \mathcal{K}} \lambda_i \zeta_{ik}(\alpha, P_{a,k})} \quad (52)$$

which is not affected by  $p_k^{\text{FD}}$ , resulting in  $\frac{\partial S_k^o}{\partial p_k^{\text{FD}}} = 0$  for  $P_{u,k} = 0$ . Hence, we can see that for  $0 \leq P_{u,k} \leq P_{a,k}$ ,  $\frac{\partial S_k^o}{\partial p_k^{\text{FD}}}$  decreases as  $P_{u,k}$  decreases and converges to 0, i.e.,  $\frac{\partial S_k^o}{\partial p_k^{\text{FD}}} \geq 0$ . Therefore,  $S_k$  is an increasing function with  $p_k^{\text{FD}}$ ,  $\forall k \in \mathcal{K}$  and the optimal  $p_k^{\text{FD}}$  that maximizes  $S_k$  is the maximum value of  $p_k^{\text{FD}}$ , which is equal to  $p_k^{\text{FD}} = 1$ .

## REFERENCES

- [1] A. Sabharwal, P. Schniter, D. Guo, D. W. Bliss, S. Rangarajan, and R. Wichman, "In-band full-duplex wireless: Challenges and opportunities," *IEEE J. Sel. Areas Commun.*, 2014, to appear.
- [2] A. Sahai, G. Patel, and A. Sabharwal, "Asynchronous full-duplex wireless," in *Proc. IEEE Int. Conf. on Commun. Systems and Networks*, Bangalore, Jan. 2010, pp. 1–9.
- [3] H. Ju, S. Lim, D. Kim, H. Poor, and D. Hong, "Full duplexity in beamforming-based multi-hop relay networks," *IEEE J. Sel. Areas Commun.*, vol. 30, no. 8, pp. 1554–1565, Sep. 2012.
- [4] Q. Li, K. Li, and K. Teh, "Achieving optimal diversity-multiplexing tradeoff for full-duplex MIMO multihop relay networks," *IEEE Trans. Inf. Theory*, vol. 57, no. 1, pp. 303–316, Dec. 2011.
- [5] B. P. Day, A. R. Margetts, D. W. Bliss, and P. Schniter, "Full-duplex MIMO relaying: Achievable rates under limited dynamic range," *IEEE J. Sel. Areas Commun.*, vol. 30, no. 8, pp. 1541–1553, Sep. 2012.
- [6] H. Ju, E. Oh, and D. Hong, "Catching resource-devouring worms in next-generation wireless relay systems: Two-way relay and full-duplex relay," *IEEE Commun. Mag.*, vol. 47, no. 9, pp. 58–65, Oct. 2009.
- [7] B. Day, A. Margetts, D. Bliss, and P. Schniter, "Full-duplex bidirectional MIMO: Achievable rates under limited dynamic range," *IEEE Trans. Signal Process.*, vol. 60, no. 7, pp. 3702–3713, Jul. 2012.
- [8] P. Weeraddana, M. Codreanu, M. Latva-aho, and A. Ephremides, "On the effect of self-interference cancellation in multihop wireless networks," *EURASIP Journal on Wireless Communications and Networking*, vol. 2010, pp. 1–10, Oct. 2010.
- [9] S. Barghi, A. Khojastepour, K. Sundaresan, and S. Rangarajan, "Characterizing the throughput gain of single cell MIMO wireless systems with full duplex radios," in *Proc. IEEE Int. Symp. on Modeling and Optimization in Mobile, Ad Hoc and Wireless Networks*, Paderborn, Germany, May 2012, pp. 68–74.
- [10] A. Sahai, S. Diggavi, and A. Sabharwal, "On degrees-of-freedom of full-duplex uplink/downlink channel," in *Proc. IEEE Inf. Theory Workshop*, Sevilla, Sep. 2013, pp. 1–5.
- [11] G. Zheng, I. Krikidis, J. Li, A. Petropulu, and B. Ottersten, "Improving physical layer secrecy using full-duplex jamming receivers," *IEEE Trans. Signal Process.*, vol. 61, no. 20, pp. 4962–4974, Oct. 2013.
- [12] L. Zhang and D. Guo, "Virtual full duplex wireless broadcasting via compressed sensing," *IEEE/ACM Trans. Netw.*, vol. 5, no. 5, pp. 1659–1671, Oct. 2014.
- [13] K. Yamamoto, K. Haneda, H. Murata, and S. Yoshida, "Optimal transmission scheduling for a hybrid of full- and half-duplex relaying," *IEEE Commun. Lett.*, vol. 15, no. 3, pp. 305–307, Mar. 2011.
- [14] D. W. K. Ng, E. S. Lo, and R. Schober, "Dynamic resource allocation in MIMO-OFDMA systems with full-duplex and hybrid relaying," *IEEE Trans. Commun.*, vol. 60, no. 5, pp. 1291–1304, May 2012.
- [15] T. Riihonen, S. Werner, and R. Wichman, "Hybrid full-duplex/half-duplex relaying with transmit power adaptation," *IEEE Trans. Wireless Commun.*, vol. 10, no. 9, pp. 3074–3085, Sep. 2011.

- [16] M. Duarte and A. Sabharwal, "Full-duplex wireless communications using off-the-shelf radios: Feasibility and first results," in *Proc. Asilomar Conf. on Signals, Systems, and Computers*, Pacific Grove, CA, Nov. 2010, pp. 1558–1562.
- [17] T. Snow, C. Fultom, and W. Chappell, "Transmit–receive duplexing using digital beamforming system to cancel self-interference," *IEEE Trans. Microw. Theory Tech.*, vol. 59, no. 12, pp. 3494–3503, Dec. 2011.
- [18] P. Lioliou, M. Viberg, M. Coldrey, and F. Athley, "Self-interference suppression in full-duplex mimo relays," in *Proc. Asilomar Conf. on Signals, Systems, and Computers*, Pacific Grove, CA, Nov. 2010, pp. 658–662.
- [19] T. Riihonen, S. Werner, and R. Wichman, "Mitigation of loopback self-interference in full-duplex MIMO relays," *IEEE Trans. Signal Process.*, vol. 59, no. 12, pp. 5983–5993, Dec. 2011.
- [20] L. Anttila, D. Korpi, E. Antonio-Rodríguez, R. Wichman, and M. Valkama, "Modeling and efficient cancellation of nonlinear self-interference in MIMO full-duplex transceivers," 2014, available at <http://arxiv.org/abs/1406.0671>.
- [21] M. Duarte, C. Dick, and A. Sabharwal, "Experiment-driven characterization of full-duplex wireless systems," *IEEE Trans. Wireless Commun.*, vol. 11, no. 12, pp. 4296–4307, Nov. 2012.
- [22] J. I. Choi, M. Jain, K. Srinivasan, P. Levis, and S. Katti, "Achieving single channel, full duplex wireless communication," in *Proc. ACM Mobicom*, Chicago, IL, Sep. 2010, pp. 1–12.
- [23] M. Jain, J. I. Choi, T. Kim, D. Bharadia, S. Seth, K. Srinivasan, P. Levis, S. Katti, and P. Sinha, "Practical, real-time, full duplex wireless," in *Proc. ACM Mobicom*, Las Vegas, NV, Sep. 2011, pp. 301–312.
- [24] D. Bharadia, E. McMillin, and S. Katti, "Full duplex radios," in *Proceedings of ACM SIGCOMM*, Hong Kong, Aug. 2013, pp. 375–386.
- [25] T. Riihonen and R. Wichman, "Analog and digital self-interference cancellation in full-duplex MIMO-OFDM transceivers with limited resolution in A/D conversion," in *Proc. Asilomar Conf. on Signals, Systems, and Computers*, Pacific Grove, CA, Nov. 2012, pp. 45–49.
- [26] Y. Hua, Y. Ma, P. Liang, and A. Cirik, "Breaking the barrier of transmission noise in full-duplex radio," in *Proc. Military Commun. Conf.*, San Diego, CA, Nov. 2013, pp. 1558–1553.
- [27] C. Cox and E. Ackerman, "Demonstration of a single-aperture, full-duplex communication system," in *Proc. IEEE Radio and Wireless Symposium*, Austin, TX, Jan. 2013, pp. 148–150.
- [28] M. Knox, "Single antenna full duplex communications using a common carrier," in *Proc. IEEE Wireless and Microwave Technology Conference*, Cocoa Beach, FL, Apr. 2012, pp. 1–6.
- [29] S. Goyal, P. Liu, S. Hua, and S. Panwar, "Analyzing a full-duplex cellular system," in *Proc. Conf. on Inform. Sci. and Sys.*, Baltimore, MD, Mar. 2013, pp. 1–6.
- [30] Z. Tong and M. Haenggi, "Throughput analysis for wireless networks with full-duplex radios," Sep. 2014, pp. 1–5, submitted, available at <http://arxiv.org/abs/1409.7433>.
- [31] T. Q. S. Quek, G. de la Roche, I. Guvenc, and M. Kountouris, *Small Cell Networks: Deployment, PHY Techniques, and Resource Allocation*. Cambridge Univ Pr, 2013.
- [32] W. C. Cheung, T. Q. S. Quek, and M. Kountouris, "Throughput optimization in two-tier femtocell networks," *IEEE J. Sel. Areas Commun.*, vol. 30, no. 3, pp. 561–574, Apr. 2012.
- [33] H. S. Dhillon, R. K. Ganti, F. Baccelli, and J. G. Andrews, "Modeling and analysis of K-tier downlink heterogeneous cellular networks," *IEEE J. Sel. Areas Commun.*, vol. 30, no. 3, pp. 550–560, Apr. 2012.
- [34] T. D. Novlan, H. S. Dhillon, and J. G. Andrews, "Analytical modeling of uplink cellular networks," *IEEE Trans. Wireless Commun.*, vol. 12, no. 6, pp. 2669–2679, Jun. 2013.
- [35] H. Dhillon, R. Ganti, and J. Andrews, "Load-aware modeling and analysis of heterogeneous cellular networks," *IEEE Trans. Wireless Commun.*, vol. 12, no. 4, pp. 1666–1677, Apr. 2013.
- [36] D. Lopez-Perez, I. Guvenc, G. de la Roche, M. Kountouris, T. Q. S. Quek, and J. Zhang, "Enhanced inter-cell interference coordination challenges in heterogeneous networks," *IEEE Commun. Mag.*, vol. 18, no. 3, pp. 22–30, Jun. 2011.
- [37] J. Lee, J. G. Andrews, and D. Hong, "Spectrum-sharing transmission capacity with interference cancellation," *IEEE Trans. Commun.*, vol. 61, no. 1, pp. 76–86, Jan. 2013.
- [38] K. Huang, V. K. N. Lau, and Y. Chen, "Spectrum sharing between cellular and mobile ad hoc networks: transmission-capacity trade-off," *IEEE J. Sel. Areas Commun.*, vol. 27, no. 7, pp. 1256–1267, Aug. 2009.
- [39] J. Lee, J. G. Andrews, and D. Hong, "Spectrum-sharing transmission capacity," *IEEE Trans. Wireless Commun.*, vol. 10, no. 9, pp. 3053–3063, Sep. 2011.
- [40] M. Wildemeersch, T. Q. S. Quek, C. H. Slump, and A. Rabbachin, "Cognitive small cell networks: Energy efficiency and trade-offs," *IEEE Trans. Commun.*, vol. 61, no. 9, pp. 4016–4029, Sep. 2013.
- [41] Y. S. Soh, T. Q. S. Quek, M. Kountouris, and H. Shin, "Energy efficient heterogeneous cellular networks," *IEEE J. Sel. Areas Commun.*, vol. 31, no. 5, pp. 840–850, May 2013.
- [42] H.-S. Jo, Y. J. Sang, P. Xia, and J. Andrews, "Heterogeneous cellular networks with flexible cell association: A comprehensive downlink SINR analysis," *IEEE Trans. Wireless Commun.*, vol. 11, no. 10, pp. 3484–3495, Oct. 2012.
- [43] S. Singh, H. S. Dhillon, and J. G. Andrews, "Offloading in heterogeneous networks: Modeling, analysis, and design insights," *IEEE Trans. Wireless Commun.*, vol. 12, no. 5, pp. 2484–2497, May 2013.
- [44] S. Soh, T. Q. S. Quek, M. Kountouris, and G. Caire, "Cognitive hybrid division duplex for two-tier femtocell networks," *IEEE Trans. Wireless Commun.*, vol. 12, no. 10, pp. 4852–4865, Oct. 2013.
- [45] M. Z. Win, P. C. Pinto, and L. A. Shepp, "A mathematical theory of network interference and its applications," *Proc. IEEE*, vol. 97, no. 2, pp. 205–230, Feb. 2009.
- [46] P. C. Pinto and M. Z. Win, "Communication in a Poisson field of interferers – Part I: Interference distribution and error probability," *IEEE Trans. Wireless Commun.*, vol. 9, no. 7, pp. 2176–2186, Jul. 2010.
- [47] P. C. Pinto and M. Z. Win, "Communication in a Poisson field of interferers – Part II: Channel capacity and interference spectrum," *IEEE Trans. Wireless Commun.*, vol. 9, no. 7, pp. 2187–2195, Jul. 2010.
- [48] J. Lee, A. Conti, A. Rabbachin, and M. Z. Win, "Distributed network secrecy," *IEEE J. Sel. Areas Commun.*, vol. 31, no. 9, pp. 1889–1900, Sep. 2013.
- [49] R. Heath, M. Kountouris, and T. Bai, "Modeling heterogeneous network interference using Poisson point processes," *IEEE Trans. Signal Process.*, vol. 61, no. 16, pp. 4114–4126, Aug. 2013.
- [50] M. Z. Win, A. Rabbachin, J. Lee, and A. Conti, "Cognitive network secrecy with interference engineering," *IEEE Netw.*, vol. 28, no. 5, pp. 86–90, Sep./Oct. 2014.
- [51] J. Bang, J. Lee, S. Kim, and D. Hong, "An efficient relay selection strategy for random cognitive relay networks," *IEEE Trans. Wireless Commun.*, 2015, to appear.
- [52] S. Akoum and R. W. Heath Jr, "Interference coordination: Random clustering and adaptive limited feedback," *IEEE Trans. Signal Process.*, vol. 61, no. 7, pp. 1822–1834, Apr. 2013.
- [53] V. Garcia, Y. Zhou, and J. Shi, "Coordinated multipoint transmission in dense cellular networks with user-centric adaptive clustering," *IEEE Trans. Wireless Commun.*, vol. 13, no. 8, pp. 4297–4308, Aug. 2014.
- [54] H. Dhillon, Y. Li, P. Nuggehalli, Z. Pi, and J. G. Andrews, "Fundamentals of heterogeneous cellular networks with energy harvesting," *IEEE Trans. Wireless Commun.*, vol. 13, no. 5, pp. 2782–2797, May 2014.
- [55] C. H. M. De Lima, M. Bennis, K. Ghaboosi, and M. Latva-aho, "Interference management for self-organized femtocells towards green networks," in *Proc. IEEE Int. Symp. on Personal, Indoor and Mobile Radio Commun.*, Istanbul, Turkey, Sep. 2010, pp. 352–356.
- [56] D. Kim, H. Ju, S. Park, and D. Hong, "Effects of channel estimation error on full-duplex two-way networks," *IEEE Trans. Veh. Technol.*, vol. 62, no. 9, pp. 4666–4672, Nov. 2013.
- [57] A. C. Cirik, Y. Rong, and Y. Hua, "Achievable rates of full-duplex MIMO radios in fast fading channels with imperfect channel estimation," *IEEE Trans. Signal Process.*, vol. 62, no. 15, pp. 3874–3886, Aug. 2014.
- [58] G. Bolch, S. Greiner, H. d. Meer, and K. S. Trivedi, *Queueing Networks and Markov Chains: Modeling and Performance Evaluation with Computer Science Applications*. Wiley-Blackwell, 2006.
- [59] I. S. Gradshteyn and I. M. Ryzhik, *Table of Integrals, Series, and Products*, 7th ed. San Diego, CA: Academic Press, Inc., 2007.
- [60] J. F. Kingman, *Poisson Processes*. Oxford University Press, 1993.



**Jemin Lee** (S'06-M'11) is a Temasek Research Fellow at the Singapore University of Technology and Design (SUTD), Singapore. She received the B.S. (with high honors), M.S., and Ph.D. degrees in Electrical and Electronic Engineering from Yonsei University, Seoul, Korea, in 2004, 2007, and 2010, respectively. She was a Postdoctoral Fellow at the Massachusetts Institute of Technology (MIT), Cambridge, MA from Oct. 2010 to Oct. 2013, and a Visiting Ph.D. Student at the University of Texas at Austin, Austin, TX from Dec. 2008 to Dec.

2009. Her current research interests include physical layer security, wireless security, heterogeneous networks, cognitive radio networks, and cooperative communications.

Dr. Lee is currently an Editor for the IEEE TRANSACTIONS ON WIRELESS COMMUNICATIONS and the IEEE COMMUNICATIONS LETTERS, and served as a Guest Editor of the Special Issue on Heterogeneous and Small Cell Networks for the ELSEVIER PHYSICAL COMMUNICATION in 2013. She also served as a Co-Chair of the IEEE 2013 Globecom Workshop on Heterogeneous and Small Cell Networks, and Technical Program Committee Member for numerous IEEE conferences. She is currently a reviewer for several IEEE journals and has been recognized as an Exemplary Reviewer of IEEE COMMUNICATIONS LETTERS and IEEE WIRELESS COMMUNICATION LETTERS for recent several years. She received the IEEE ComSoc Asia-Pacific Outstanding Young Researcher Award in 2014, the Temasek Research Fellowship in 2013, the Chun-Gang Outstanding Research Award in 2011, and the IEEE WCSP Best Paper Award in 2014.



**Tony Q.S. Quek** (S'98-M'08-SM'12) received the B.E. and M.E. degrees in Electrical and Electronics Engineering from Tokyo Institute of Technology, Tokyo, Japan, respectively. At Massachusetts Institute of Technology, he earned the Ph.D. in Electrical Engineering and Computer Science. Currently, he is an Assistant Professor with the Information Systems Technology and Design Pillar at Singapore University of Technology and Design (SUTD). He is also a Scientist with the Institute for Infocomm Research.

His main research interests are the application of mathematical, optimization, and statistical theories to communication, networking, signal processing, and resource allocation problems. Specific current research topics include sensor networks, heterogeneous networks, green communications, smart grid, wireless security, compressed sensing, big data processing, and cognitive radio.

Dr. Quek has been actively involved in organizing and chairing sessions, and has served as a member of the Technical Program Committee as well as symposium chairs in a number of international conferences. He is serving as the PHY & Fundamentals Track for IEEE WCNC in 2015, the Communication Theory Symposium for IEEE ICC in 2015, and the PHY & Fundamentals Track for IEEE EuCNC in 2015. He is currently an Editor for the IEEE TRANSACTIONS ON COMMUNICATIONS, the IEEE WIRELESS COMMUNICATIONS LETTERS, and an Executive Editorial Committee Member for the IEEE TRANSACTIONS ON WIRELESS COMMUNICATIONS. He was Guest Editor for the IEEE SIGNAL PROCESSING MAGAZINE (Special Issue on Signal Processing for the 5G Revolution) in 2014, and the IEEE WIRELESS COMMUNICATIONS MAGAZINE (Special Issue on Heterogeneous Cloud Radio Access Networks) in 2015.

Dr. Quek was honored with the 2008 Philip Yeo Prize for Outstanding Achievement in Research, the IEEE Globecom 2010 Best Paper Award, the CAS Fellowship for Young International Scientists in 2011, the 2012 IEEE William R. Bennett Prize, the IEEE SPAWC 2013 Best Student Paper Award, and the IEEE WCSP 2014 Best Paper Award.